

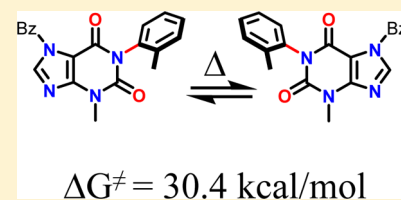
Conformational Analysis and Absolute Configuration of Axially Chiral 1-Aryl and 1,3-Bisaryl-xanthines

Michele Mancinelli,*¹ Sofia Perticarari, Luca Prati, and Andrea Mazzanti*²

Department of Industrial Chemistry "Toso Montanari", University of Bologna, Viale Risorgimento 4, 40136 Bologna, Italy

S Supporting Information

ABSTRACT: The xanthine scaffold is known to be the forefather of a class of biological active molecules. Xanthine is a planar framework in which an aryl substituent linked in the 1 or 3 position is driven out of the xanthine plane because of the steric hindrance exerted by the two carbonyls. This work analyses the stereodynamics of some 1-aryl and 1,3-bisaryl-xanthines and describes the steric requirements needed to produce stable heteroaromatic atropisomers or diastereoisomers, with one or two N-C_{sp2} stereogenic axes. The N-C racemization barrier was found to be bigger than 25 kcal/mol. The absolute configurations of the novel atropisomers has been assigned using TD-DFT simulation of ECD spectra.



INTRODUCTION

The optical activity generated by a chiral axis was first recognized by Christie and Kenner in 1922.¹ Later, the term "atropisomerism" was coined by Kuhn in 1933² and its definition was refined by Oki.³ This phenomenon has been largely overlooked as a source of stereoisomerism alternative to classical stereogenic centers for many decades. This situation changed first with the preparation of atropisomeric catalysts⁴ and then with the discovery of many bioactive natural compounds containing stereogenic axes.⁵ More recently, Clayden and La Plante underlined the pharmaceutical implications of atropisomerism in drug discovery.^{6–8}

Barbiturates are the most studied class of biologically active compounds having a C_{sp2}-N stereogenic axis,⁹ but also lactams,¹⁰ imides,¹¹ oxazolindione¹² and thiazolidine-2-thiones¹³ and their derivatives show characteristic N-aryl chiral axes (Figure 1) and some organocatalytic atroposelective syntheses have been recently reported.¹⁴

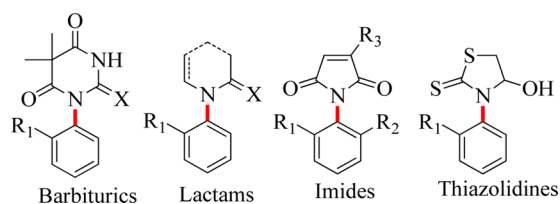


Figure 1. Atropisomeric compounds bearing an N-aryl chiral axis.

Modified purine bases play an important role in biology, and they are interesting systems under biochemical, pharmacological, and chemical points of view. Xanthines, in particular, exists in both prokaryote and eukaryote cells and participates in a large variety of functions in most human body tissues and fluids, and a number of central nervous system, muscles and cardiac stimulants are derived from xanthines, including caffeine and theobromine (Figure 2).

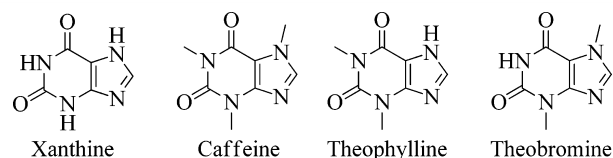


Figure 2. Natural occurring xanthines.

Despite its biological activity, poor attention has been devoted to the dynamic conformations of this scaffold because it is not possible to install an ordinary source of chirality (i.e., an asymmetric carbon) without modify one of its essential functional groups. On the other hand, it could be possible to install stereogenic axes. The xanthine backbone is a planar framework in which an aryl substituent linked in the 1 or 3 position is driven out of the xanthine plane because of the steric hindrance caused by the two carbonyls. If the aryl ring has not C₂ local symmetry, the out-of-plane displacement implies the formation of conformational chirality. Depending on the steric features of the aryl substituent, the resulting conformational enantiomers are expected to be either stereo labile or configurationally stable (atropisomers).

This work aims to investigate the stereodynamics of a class of 1-aryl and 1,3-bisaryl-xanthines and to evaluate the steric requirements needed to produce stable heteroaromatic atropisomers or diastereoisomers with one or two C_{sp2}-N stereogenic axes.¹⁵ With those parameters in hands, it is possible to design and prepare axially chiral xanthines, whose enantiomers are stable at ambient temperature and can eventually have application in drug discovery.

Received: April 27, 2017

Published: June 13, 2017

RESULTS AND DISCUSSION

The unique X-ray structure for a 1-phenyl xanthine¹⁶ shows that the phenyl ring is displaced by 79.5° with respect to the xanthine plane, and no X-ray structures are known for 3-aryl xanthines. If the aryl ring lacks a local C₂ axis of symmetry (i.e., it has an *ortho* or *meta* substituent), its skewed arrangement implies the formation of a pair of conformational enantiomers, whose conformational stability depends on the steric hindrance of the aryl *ortho* substituent. When a second asymmetric aryl ring is linked to the second nitrogen of the six-membered ring, the combination of the two stereogenic axes lead to the formation of four stereoisomers (see Figure 3). They can be

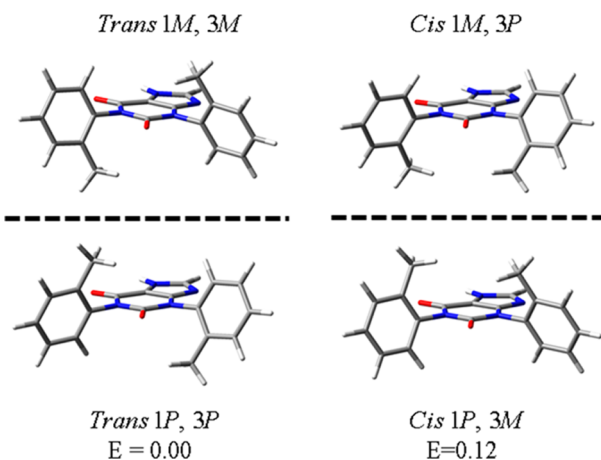


Figure 3. Four available stereoisomers of the model compound (energy values in kcal/mol, calculated at the B3LYP/6-31G(d) level of theory).

conveniently named as *cis* when the two *ortho*-substituents are on the same side, and *trans* when the two *ortho*-substituents are on opposite side with respect to the plane of xanthine.

Preliminary theoretical studies were performed to forecast the conformational preferences and to estimate the rotational barriers involved. The *ortho*-tolyl moiety was chosen as a prototype of the aryl rings linked in positions 1 and 3 of the xanthine scaffold. The four conceivable stereoisomers were optimized at the B3LYP/6-31G(d) level of theory and the stationary points were validated by frequency analysis. Despite the presence of an *ortho*-substituent, DFT calculations suggested that the two aryl rings are not exactly perpendicular to the xanthine scaffold, so an additional conformation has to be considered for each aryl ring, yielding a total of eight diastereomeric conformations. However, the energy differences among the four conformations of each stereoisomer are very small (less than 1 kcal/mol) and only the most stable conformation of each stereoisomer are shown in Figure 3.

Four transition states must be considered to allow diastereomerization and enantiomerization (Figure 4). The *ortho*-methyl group of the ring in position 1 can rotate over the carbonyl in position 9 or over the carbonyl in position 2. On the other side, the *ortho*-methyl of the 3-aryl ring can rotate over the 2-carbonyl or over the nitrogen in position 5. The values of energy barriers, derived after optimization with DFT at the B3LYP/6-31G(d) level, suggest a lower barrier for the rotation of the 3-aryl group with respect to the rotation of the 1-aryl (Table 1), where the steric constraints imposed by the two carbonyls are more severe. The two barriers are separated by a relatively large energy gap (3.5 kcal/mol), so they should

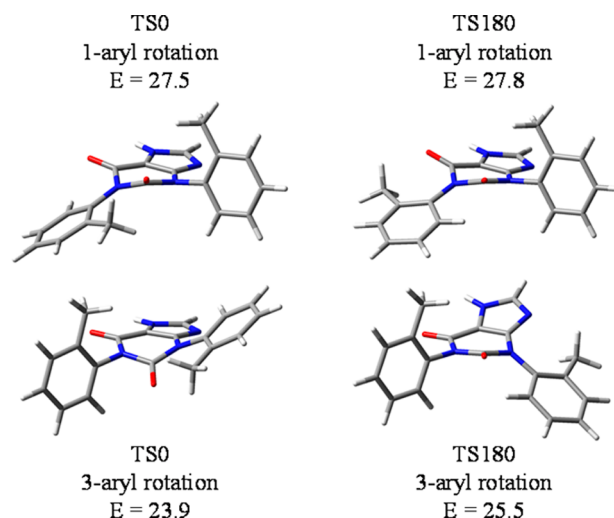


Figure 4. Four available transition states for the model compound (energy values in kcal/mol, at the B3LYP/6-31G(d) level of theory).

Table 1. Calculated Energy Barriers for Rotations of 1-Tolyl and 3-Tolyl Rings (Values in kcal/mol at the B3LYP/6-31G(d) Level of Theory)

	1-aryl, TS0	1-aryl, TS180	3-aryl, TS0	3-aryl, TS180
ΔE	27.52	27.84	23.93	25.48
ΔH°	27.03	27.32	23.48	24.96

be independently observed. In both cases (1-aryl and 3-aryl rotation) the suggested energy barriers are quite high, amenable to develop stable atropisomers at ambient temperature and above, thus making these compounds suitable for biological investigation as class-3 atropisomers.⁶

To experimentally verify the results of calculations, we synthesized 1-aryl and 1,3-bisaryl-xanthines 1–9 (Figure 5) following two different synthetic approaches (see Experimental section and Figure S1–S2 of SI for details).

A well-known method to detect the existence of a pair of conformationally unstable atropisomers is dynamic-NMR spectroscopy.¹⁷ While the presence of diastereomeric conformations in 1,3-bisaryl-xanthines is straightforwardly detected by standard NMR analysis, the occurrence of enantiomeric

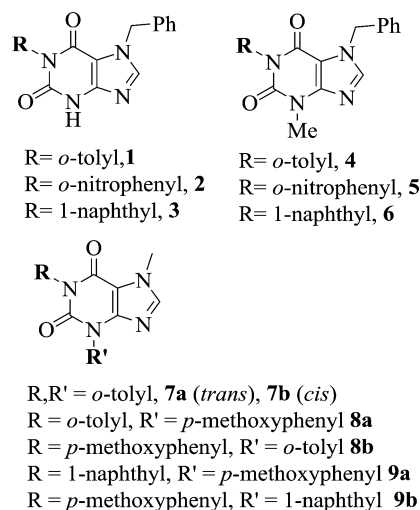


Figure 5. 1-Aryl and 1,3-bisaryl-xanthines.

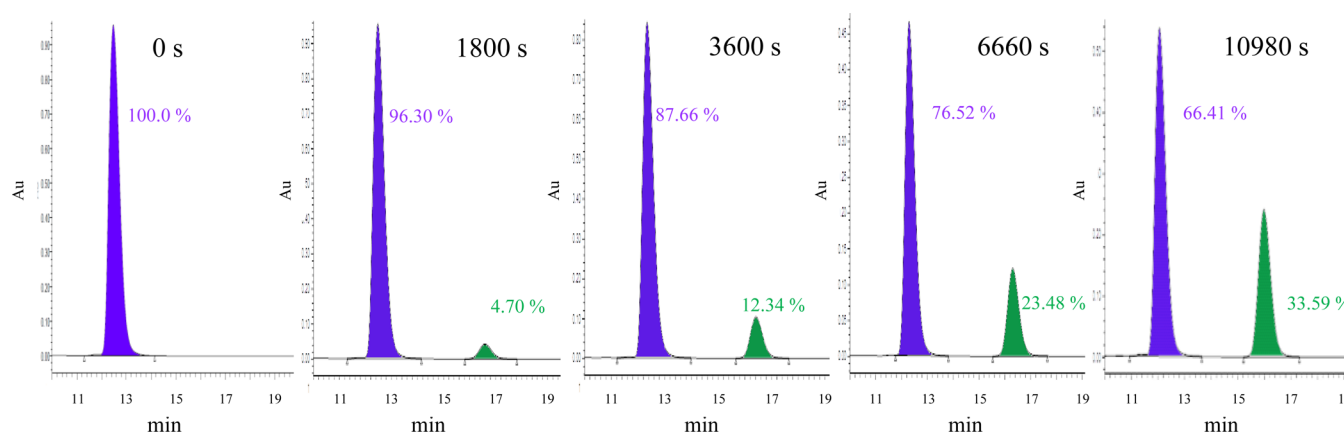


Figure 6. Example of racemization of compound 4 followed by CSP-HPLC. Times are referred to the sample kept at +115 °C in C₂D₂Cl₄.

conformations (compounds 1–6) could be revealed by using a Chiral Solvating Agent (CSA) such as Pirkle’s alcohols, or by the presence of a chirality probe containing two geminal groups that show diastereotopic signals when conformational enantiomers are formed. To avoid the drawbacks that hamper the use of CSAs at high temperatures, a benzyl group was added in position 7 of the xanthine core to be used as chirality probe. This group was chosen for the presence of an uncoupled CH₂ group that is a singlet when the motion is fast, and it splits into diastereotopic signals (AB system) when the enantiomerization process is frozen in NMR time scale.

1-Aryl Xanthines. The presence of the chirality probe widens the conformational space available. Depending on the relative disposition of the benzyl group with respect to the *ortho*-substituent of the 1-aryl ring, two different conformations are produced: they can be named as *syn* and *anti*. The *syn* conformation has the phenyl ring of the benzyl group on the same side of the *ortho* substituent of the 1-aryl ring with respect to the xanthine core, whereas in the *anti* conformation the phenyl of the benzyl group is on the opposite side of the *ortho*-substituent of the 1-aryl ring (see Figures S3–S8 and Table S1 of SI).

The ambient temperature NMR spectrum of compound 1 showed the expected AB system for the benzyl signal, and when the sample was heated to +120 °C (Figure S9 in SI), no line broadening was observed, thus suggesting a very high rotational barrier. Preliminary HPLC tests were performed on compound 1 by using enantioselective amylose- and cellulose-based columns. The best results (Figure S10 in SI) were obtained on ChiralPak AD-H chiral stationary phase (CSP). Unfortunately, the presence of the NH in position 3 lead to heavily broadened chromatographic peaks, probably because of its interaction with the stationary phase. To solve this issue the NH was protected with a methyl group (compounds 4–6, see Experimental Section for details) that does not interfere with the rotation around the chiral axis. This allowed to a good separation with well resolved chromatographic peaks (see Figure S11–S13 in SI). A semipreparative approach was used to resolve the atropisomer in the 10 mg scale.

The racemization process was followed by means of CSP-HPLC (Figure 6 for compound 4 and Figure S14–S16 for compounds 4–6), keeping an enantiopure sample at high temperature in C₂D₂Cl₄ and collecting aliquots that were analyzed using the same elution conditions used in the purification step (see Experimental Section for details). Once complete racemization was reached, the experimental values of

ΔG^\ddagger were derived by a first order reversible kinetic equation (Table S2 in SI). Taking into account the errors in the determination of the sample temperature (± 2 °C), the free energies can be considered invariant with the temperature, thus implying a very small (or negligible) activation entropy.¹⁷ The experimental values of compounds 4–6 have racemization barriers high enough to ensure very long racemization times at ambient and human-body temperatures (“class 3” in LaPlante’s scheme).⁶ Table 2 summarizes the experimental and calculated values for compounds 4–6.

Table 2. Experimental and Computed Energy Barriers for Racemization Around the 1-Aryl Stereogenic Axis, and Corresponding Half-Lifetimes (Energy Values in kcal/mol)

compd.	$\Delta G^\ddagger_{\text{exp}}$	$\Delta G^\ddagger_{\text{calc}}$	$t_{1/2}$ (+25 °C)	$t_{1/2}$ (+37 °C)
4	30.5	28.1	82 y	10.8 y
5	25.4	23.8	5.4 d	1 d
6	32.5	30.5	2400 y	276 y

It should be noted that the racemization barrier of compound 5 is much smaller (of about 5.1 kcal/mol) than that of compound 4, while the methyl and the nitro group are considered isosteric.¹⁸ This difference, however, is in agreement with a stabilization of the transition state due to N–O interaction with the carbonyl groups.¹⁹

1,3-Bisaryl-xanthines. When a second *ortho*-substituted aryl ring is bound to position 3 of the xanthine core, a second stereogenic axis is generated, hence two conformational diastereoisomers (each composed by a pair of enantiomers) are conceivable. They can be conveniently named as *cis* and *trans* depending on the relative disposition of the two *ortho*-substituents of the aryl rings with respect to the xanthine core. DFT calculations had suggested (see Figure 3) that the ground state energies of the two diastereoisomers are very similar, thus both diastereoisomers should be appreciably populated. As in the case of compounds 1–6, the aryl rings are not exactly perpendicular to the xanthine ring, thus providing more conformations to be considered in the conformational analysis. Figure 7 reports the lowest energy conformations for the *cis* and *trans* diastereoisomer of compound 7.

The two diastereoisomers can be converted into each other by the rotation of one of the two aryl rings. DFT optimization of the four conceivable transition states suggest that the rotational barrier of the aryl ring in position 3 is lower than the one in position 1 by 2.1 kcal/mol (Table S3 in SI). The

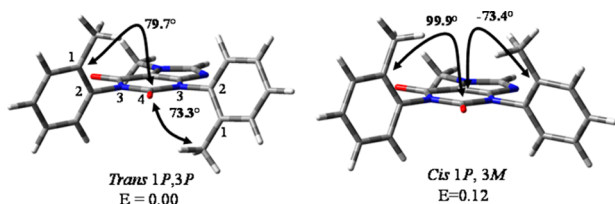


Figure 7. Lowest energy conformation for *cis* and *trans* diastereoisomers of compound **7** (energy values in kcal/mol, at the B3LYP/6-31G(d) level of theory).

rotation of the 3-aryl ring should therefore yield diastereomerization, while rotation of the 1-aryl ring should yield racemization. Compounds **7–9** were prepared by a multistep synthesis (see details in the [Experimental Section](#) and in [SI](#)) starting from 1,3-bisaryl-barbiturates. In these compounds the 7-benzyl group (i.e., the chirality probe) is not required for the stereodynamic analysis, and it was conveniently replaced with a methyl in the last reaction step (this eliminates the issues in the resolution of the stereoisomers by HPLC, as observed in compounds **1–3**).

The two diastereoisomers of **7** were observed in the NMR spectrum at ambient temperature in a 57:43 ratio ([Figure S17](#)), and the four conformational stereoisomers were completely resolved at ambient temperature on amylose-based CSP-HPLC column (Chiralpak AD-H, [Figure 8](#)). Samples in the 10 mg scale were obtained by a semipreparative approach.

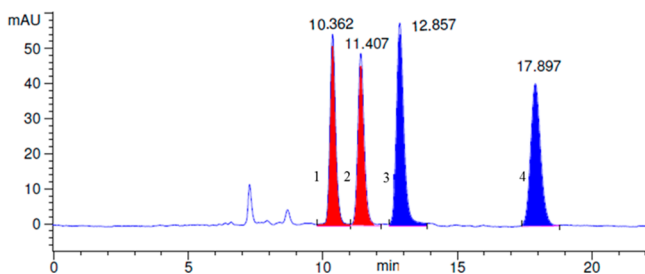


Figure 8. HPLC chromatogram of **7** (Chiralpak AD-H, 10 μ m, 250 \times 20 mm, 20 mL/min hexane/*i*PrOH 80/20 v/v).

NMR analysis allowed to assign the first two peaks (red in [Figure 8](#)) to one diastereoisomer and the last two peaks (blue in [Figure 8](#)) to the second one. NOE-NMR experiments were then employed to determine the relative disposition of the two *ortho*-tolyl rings. DFT optimized structure for the *cis* diastereoisomer suggests that the two methyls are sufficiently close to yield reciprocal NOE effect, while in the *trans* diastereoisomer the two methyls are too far away to produce any NOE enhancement. Since the methyls have different chemical shifts, the saturation of one methyl of the *cis* diastereoisomer should yield NOE enhancement on the other. Unfortunately the two methyl signals have very similar chemical shifts in both isomers ($\Delta\nu < 10$ Hz, [Figure S14](#)) and the standard technique is not applicable. Using a different approach,²⁰ we simultaneously saturated the ^{13}C satellites of both methyls to observe NOE on the $^{12}\text{CH}_3$ signals ([Figure 9](#)). The experiment performed on the third and fourth eluted stereoisomers yielded noticeable NOE, while the first and second eluted stereoisomers did not show any enhancement. It was then straightforward to assign the 3 + 4 pair to the *cis* diastereoisomer (**7b**) and the 1 + 2 pair to the *trans* one (**7a**).

The diastereomerization rates were measured at +77 $^\circ\text{C}$ and +82 $^\circ\text{C}$ with NMR starting from an enantiopure sample of **7** in DMSO. The ^1H NMR spectra were acquired at fixed times and the diastereomeric ratios were fitted using a first-order-kinetic, (see [Figure S18](#) in [SI](#)) yielding a ΔG^\ddagger value of 26.0 kcal/mol. The higher rotational barrier (enantiomerization) was measured by keeping at high temperature (+105 $^\circ\text{C}$, +110 $^\circ\text{C}$ and +115 $^\circ\text{C}$ in $\text{C}_2\text{D}_2\text{Cl}_4$) the same sample containing the two equilibrated diastereoisomers,²¹ having the same helicity at the second chiral axis. Aliquots were collected during the time and analyzed at ambient temperature by HPLC, monitoring the growth of the other two diastereoisomers and summing up their intensities (see [Figure S19](#) in [SI](#)). The first-order kinetic fitting yielded a $\Delta G^\ddagger = 30.4$ kcal/mol. Within the experimental errors, this value is identical to that measured for compound **4** ([Table S2 SI](#)). This equivalence confirms that the higher barrier corresponds to the rotation of 1-*ortho*-tolyl, while the lower diastereomerization barrier is that of the 3-aryl group, as suggested also by DFT calculations. [Table 3](#) summarizes the results obtained for compounds **7–9** (details in [Figures S20–S23](#) of [SI](#)).

Absolute Configuration. Once the stereodynamic behavior and thus the conformational stability of each atropisomeric structure has been analyzed, we pursued the determination of their absolute configuration. In the present cases the molecules do not contain any heavy atom suitable for the assignment by anomalous dispersion X-ray crystallography. Instead, the theoretical calculation of electronic circular dichroism (ECD) spectra by TD-DFT calculations was selected for the absolute configuration assignment of compounds **4–9**.^{22,23}

Compound **6** was selected as prototype for the AC assignment of the 1-aryl compounds. The conformational search had suggested that compound **6** has two populated conformations (*syn* and *anti*), depending on the position of the benzyl compared to the naphthyl keeping in account the planar xanthine core.

The ECD spectrum of the second eluted atropisomer of **6** shows a broad negative band centered at 278 nm, and two strong opposite Cotton effects at 226 nm (positive) and 208 nm (negative) ([Figure 10](#)). The electronic excitation energies and rotational strengths were calculated for the *syn* and *anti* conformations in the gas phase using the geometries optimized at the B3LYP/6-31G(d) level and using TD-DFT with four different functionals (CAM-B3LYP, BH&HLYP, M06-2X, ω B97XD)²⁴ to explore whether different theoretical models provide different shapes of the simulated spectra (see [Figure S24](#) of [SI](#)). An investigation of the molecular orbitals (MO) involved in the UV transitions that generate the ECD bands (see [Table S4](#) and [Figures S25](#) and [S26](#) of [SI](#)) confirmed that the weak band centered at 278 nm is mainly generated by MOs that involve the two carbonyls of the xanthine scaffold, with smaller contributions from MOs involving the naphthyl ring and the benzyl group. The band centered at 226 nm is due to the electronic transitions that mainly involve the MOs of the naphthyl moiety, but also of the purine scaffold. The same happens in the high energy band at 208 nm that is mainly due to MOs over naphthalene and the six-membered ring of xanthine.

The conformational ratio suggested by calculations (*syn:anti* 55:45) was used to produce the simulated ECD spectrum. The comparison between the computed ECD spectra for *M* configuration and the experimental ECD spectrum of second eluted peak is very good, and it assigns the *M* absolute

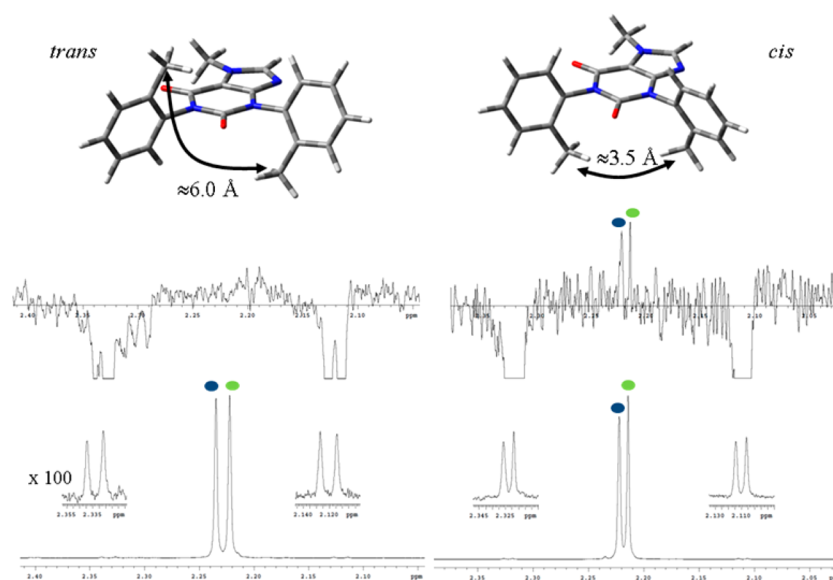


Figure 9. DPGSE-NOE for compound 7, on saturation of the ^{13}C satellites of both methyls (600 MHz in CDCl_3). Left: first eluted stereoisomer. Right: third eluted stereoisomer. Bottom: ^1H control spectra. Top: NOE spectra.

Table 3. Experimental and Computed Energy Barriers for Aryl Rotation around the Two Stereogenic Axes, and Corresponding Half Lifetime^a

compd.	1-aryl rotation		$t_{1/2}$		3-aryl rotation		$t_{1/2}$	
	ΔG^\ddagger		+25 °C	+37 °C	ΔG^\ddagger	+25 °C	+37 °C	
7	30.4 (27.5)		69.3 y	9.1 y	26.0 (23.5)	15 d	2.6 d	
8a	30.5 (27.5)		82 y	10.7 y	–	–	–	
8b	–		–	–	26.2 (23.7)	21 d	3.6 d	
9a	32.8 (30.1)		3917 y	442 y	–	–	–	
9b	–		–	–	28.4 (25.6)	2.6 y	0.4 y	

^aIn parentheses are reported the calculated values in kcal/mol (B3LYP/6-31G(d) level).

configuration to the second eluted atropisomer, while the first eluted peak has *P* absolute configuration (Figure 11).

As for compound 6, we have computed the ECD calculated spectra of the *M* atropisomer of compound 4 and 5 and compared with the experimental ECD spectra (Figures S27–S30 of SI). As a variance, compounds 4 and 5 have four ground states conformations for each atropisomer due to the nonperpendicularity of the aryl rings (see Table S1 of SI), so four ECD spectra were calculated and weighed using the relative energies suggested by calculations. For both compounds the simulation obtained for the *M* configuration is in agreement with the ECD spectrum of the first eluted atropisomer.

1,3-Bisaryl-xanthenes 7–9. The same approach was used to determine the absolute configuration of 1,3-bisaryl xanthenes 7–9. In this cases the absence of the 7-benzyl group reduces the number of conformation to be considered, and only the conformations due to the imperfect perpendicularity of the aryl rings have to be considered. As shown in Figure 8, two diastereoisomeric pairs of atropisomers were separated from the compound 7. The opposite shape of the ECD spectra of the first and second eluted atropisomers, as well as the third and fourth ones, confirmed the assignment of the atropisomeric pairs.

Starting from the relative configuration found with NOE experiments (Figure 9), the ECD spectra were calculated assuming the 1*P*,3*P* (i.e., 7a) and 1*P*,3*M* (i.e., 7b) absolute configurations and compared with the experimental ECD

spectra correspond to the second eluted atropisomer (7a) and to the third eluted one (7b, see Figure 12, further details are shown in Figures S31–S34 of SI). The absolute configurations of all compounds are summarized in the Table 4 (for compound 8 and 9 the details are reported in Figures S35–S46 of SI).

CONCLUSIONS

We have investigated, by means of DFT simulation, the opportunity to generate conformationally stable stereogenic axes directly linked to the xanthine scaffold. Once assessed the steric requisites of the substituents, we have synthesized a series of 1-aryl-xanthenes (1–6) and 1,3-bisaryl-xanthenes (7–9). The resolution of the atropisomers was performed with enantioselective HPLC. The free activation energies, determined by kinetic studies performed with NMR or CSP-HPLC, showed that these products are fully stable at ambient temperature (days to years half lifetime), and therefore usable with retention of chirality in drug discovery. The absolute configurations of all compounds was determined using TD-DFT simulation of optical spectra (ECD).

EXPERIMENTAL SECTION

Spectroscopic Data. NMR spectra were recorded using a spectrometer operating at a field of 14.4 T (600 MHz for ^1H , 150.8 for ^{13}C). Chemical shifts are given in ppm relative to the internal standard tetramethylsilane (^1H and ^{13}C) or relative to the residual peak of the solvents. The assignment of the ^{13}C signals was obtained

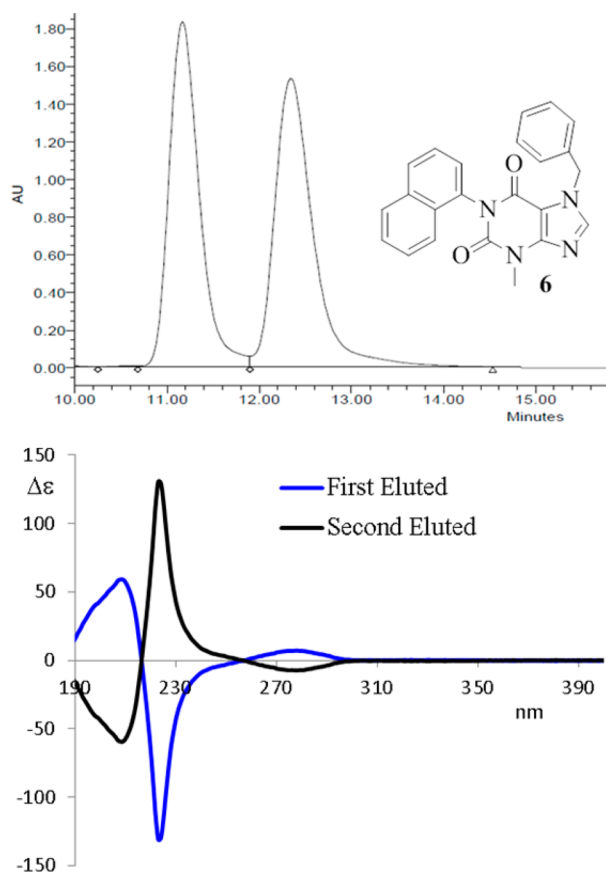


Figure 10. Top: HPLC resolution of the atropisomeric pair of compound **6** (Chiralpak AD-H, hexane/*i*PrOH 76:24). Bottom: Experimental ECD spectra recorded in acetonitrile of first eluted (blue trace) and of the second eluted (black trace).

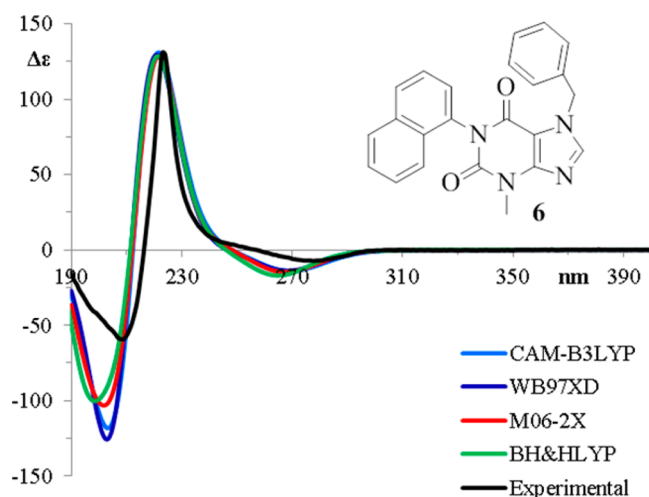


Figure 11. Experimental ECD of the second eluted atropisomer of **6** (black trace) compared to the calculated ECD for the *M* configuration with 4 different functionals (CAM-B3LYP, ω B97XD, M06-2X, BH&HLYP) and the 6-311++G(2d,p) basis set. The calculated ECD spectra are red-shifted by 10 nm, 10 nm, 10 and 14 nm and multiplied by a factor of 0.75, 0.72, 0.70, 0.80, respectively.

by means of DEPT, gs-HSQC and gs-HMBC spectra. The 150.8 MHz ^{13}C spectra were acquired under proton decoupling conditions with a 36 000 Hz spectral width, 5.5 μs (60° tip angle) pulse width, 1 s acquisition time and 5 s delay time. NOE spectra were obtained at 600

MHz using the DPFGE sequence²⁵ and a 10 Hz wide selective pulse with a R-SNOB shape.²⁶

ECD Spectra. ECD spectra were recorded at $+25^\circ\text{C}$ in far-UV HPLC-grade acetonitrile solutions. The concentrations of the samples (about 10^{-4}M) were tuned by dilution of a mother solution ($1 \times 10^{-3}\text{M}$) to obtain a maximum absorbance of about $0.8 \div 0.9$ in the UV spectrum using a 0.2 cm path length. The spectra were recorded in the 190–400 nm interval as the sum of 16 spectra.

Calculations. Ground state optimizations and transition states were obtained by DFT computations performed by the Gaussian 09 rev D.01 series of programs²⁷ using standard parameters. The calculations for ground states and transition states employed the B3LYP hybrid HF-DFT functional²⁸ and the 6-31G(d) basis set. The analysis of the vibrational frequencies for the optimized structures showed the absence of imaginary frequencies for the ground states, and the presence of one imaginary frequency for each transition state. Visual inspection of the corresponding normal mode²⁹ validated the identification of the transition states. If not differently stated, the energy values presented in the Results and Discussion section derive from total electronic energies. The ECD spectra of compounds were calculated using TD-DFT using BH&HLYP, M06-2X, ω B97XD, CAM-B3LYP and the 6-311++G(2d,p) basis set. 60 discrete transitions were calculated for each conformation (lowest calculated wavelength about 160 nm) and the ECD spectrum was obtained by convolution of Gaussian shaped lines (0.25 eV line width).²⁹ The simulated spectra resulting from the Boltzmann averaged sum of the conformations were vertically scaled and red-shifted to get the best simulations with the experimental spectra.

Racemization Rate Measurements. An aliquot of a pure enantiomer was dissolved in 1 mL of $\text{C}_2\text{D}_2\text{Cl}_4$ using a test tube with screw cap. The tube was kept into a bath of DMSO surrounded by an oil bath, placed on a hot plate magnetic stirring. The oil bath is necessary to keep the temperature controlled by means of a thermocouple put in DMSO solution. The choice of $\text{C}_2\text{D}_2\text{Cl}_4$ was made because its high boiling point, still with a good vapor pressure that allows to easily evaporate it. Small aliquotes were taken at different times, the solvent was evaporated and the sample was analyzed by enantioselective HPLC, that allowed the determination of the enantiomeric ratio at different reaction times.

Materials. Anilines, aryl-isocyanate, triethylamine, malonyl chloride, POCl_3 , CH_3NH_2 (40% aq), NaNO_2 , CH_3COOH , K_2CO_3 , CH_3I , DMF, EtOH, CHCl_3 were commercially available. THF were dried before use by distillation over Na/benzophenone. The following stationary phases were employed for the chromatography: Silica gel 60 Å F254 (Merck) for the TLC and silica gel 60 Å (230–400 mesh, Sigma-Aldrich) for atmospheric pressure chromatography. Reactions that needed anhydrous conditions were performed under a dry nitrogen flow. The glassware used in these reactions was placed in an oven at $+70^\circ\text{C}$ for at least 3 h immediately before use. Ethyl-4-amino-1-benzyl-1*H*-imidazole-5-carboxylate (CAS: 630413-89-7) was prepared as reported in the literature.³⁰

General Procedure for the Synthesis of Compounds 1–3.

The appropriate aryl isocyanate (0.4 mmol) was added to a solution of ethyl-4-amino-1-benzyl-1*H*-imidazole-5-carboxylate (0.2 mmol) in THF (4.7 mL) and the reaction mixture was stirred under reflux conditions for 7h. The resulting mixture was concentrated under reduced pressure conditions and then dissolved in 5 mL of DMF. *t*-BuOK (0.067g, 0.6 mmol) were added to this solution. The mixture was stirred under reflux overnight. Subsequently, the mixture was quenched with an aqueous solution of HCl and extracted with EtOAc. The combined organic layer was dried with Na_2SO_4 , filtered, concentrated under reduced pressure and purified by column chromatography (EtOAc:Hexane = 2:1 with gradient to 1:0) to afford products 1–3 with a 80% (white amorphous solid, 53 mg, 0.16 mmol), 65% (white amorphous solid, 47 mg, 0.13 mmol), and 80% yield (white amorphous solid, 58 mg, 0.157 mmol), respectively.

7-Benzyl-1-(*o*-tolyl)-1*H*-purine-2,6(3*H*,7*H*)-dione (1). ^1H NMR (600 MHz, CD_3CN , 1.96 ppm, $+25^\circ\text{C}$) δ 2.07 (s, 3H), 5.46 (s, 2H), 7.15 (d, $J = 7.8$ Hz, 1H), 7.29–7.38 (m, 8H), 7.85 (s, 1H), 9.87 (NH). ^{13}C NMR (150.8 MHz, CD_3CN , 118.3 ppm, $+25^\circ\text{C}$) δ 17.4

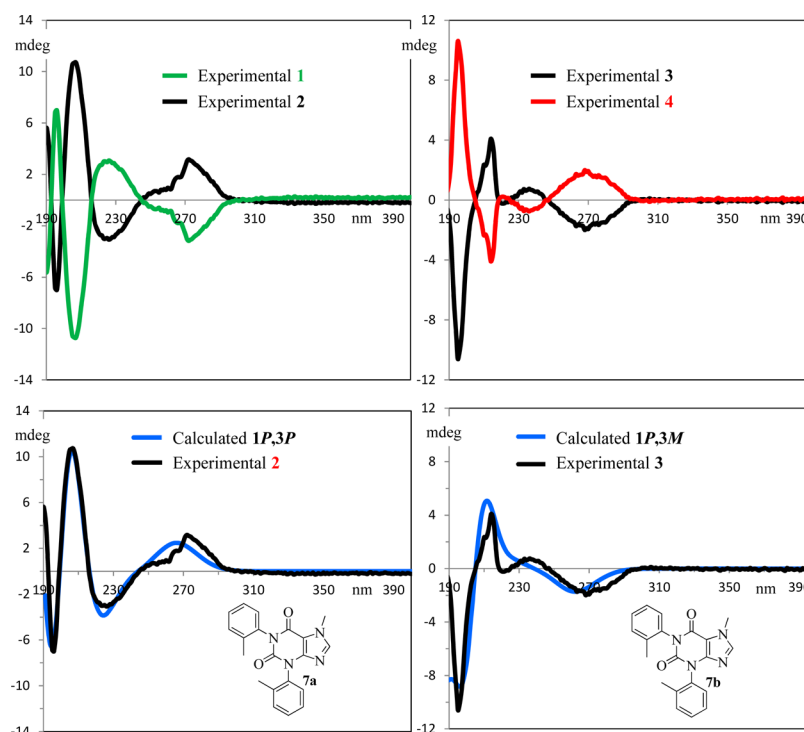


Figure 12. Top: Experimental ECD spectra in acetonitrile of the four atropisomers of **7**. Bottom: Experimental ECD spectra compared to the calculated ECD spectra (CAM-B3LYP/6-311++G(2d,p)) to the reported configuration.

Table 4. Absolute Configurations of Compounds 4–9, Derived from TD-DFT Simulation

compd	HPLC column	absolute configuration			
		1° eluted	2° eluted	3° eluted	4° eluted
4	ChiralPak AD-H	1M	1P		
5	Lux Cellulose-2	1M	1P		
6	ChiralPak AD-H	1P	1M		
7a	ChiralPak AD-H	1M, 3M	1P, 3P		
7b	ChiralPak AD-H			1P, 3M	1M, 3P
8a	ChiralPak AD-H	1M	1P		
8b	ChiralPak AD-H	3M	3P		
9a	Lux Cellulose-2	1P	1M		
9b	Lux Cellulose-2	3M	3P		

(CH₃), 50.5 (CH₂), 107.8 (Cq), 127.7 (CH), 128.7 (CH), 129.1 (CH), 129.6 (CH), 129.7₅ (CH), 130.3 (CH), 131.6 (CH), 136.1 (Cq), 137.6 (Cq), 137.8 (Cq), 143.4 (CH), 149.3 (Cq), 151.8 (Cq), 156.2 (Cq). HRMS(ESI-QTOF). Calcd for C₁₉H₁₇N₄O₂⁺ 333.1346. Found 333.1348.

7-Benzyl-1-(2-nitrophenyl)-1H-purine-2,6(3H,7H)-dione (2). Compound **2** was further purified by semipreparative HPLC on a Luna C18 column (5 μm, 250 × 21.2 mm, 20 mL/min, ACN:H₂O = 63:37 v/v). ¹H NMR (600 MHz, CD₃CN, 1.96 ppm, +25 °C) δ 5.42 (d, *J* = 15.2 Hz, 1H), 5.45 (d, *J* = 15.2 Hz, 1H), 7.32–7.38 (m, 5H), 7.52 (dd, *J* = 7.9, 1.5 Hz, 1H), 7.69 (ddd, *J* = 8.2, 7.6, 1.5 Hz, 1H), 7.84 (ddd, *J* = 7.9, 7.6, 1.5 Hz, 1H), 7.9 (s, 1H), 8.16 (dd, *J* = 8.2, 1.5 Hz, 1H), 9.52 (NH). ¹³C NMR (150.8 MHz, CD₃CN, 118.3 ppm, +25 °C) δ 50.6 (CH₂), 107.6 (Cq), 126.2 (CH), 128.6 (CH), 129.2 (CH), 129.8 (CH), 130.4 (Cq), 131.0 (CH), 133.3 (CH), 135.4 (CH), 137.5 (Cq), 144.0 (CH), 147.7 (Cq), 149.6 (Cq), 151.4 (Cq), 155.8 (Cq). HRMS(ESI-QTOF). Calcd for C₁₈H₁₄N₅O₄⁺ 364.1040. Found 364.1044.

7-Benzyl-1-(naphthalene-1-yl)-1H-purine-2,6(3H,7H)-dione (3). Compound **3** was further purified by semipreparative HPLC on a Luna C18 column (5 μm, 250 × 21.2 mm, 20 mL/min, ACN:H₂O = 90:10 v/v). ¹H NMR (600 MHz, CD₃CN, 1.96 ppm, +25 °C) δ 5.45

(d, *J* = 15.2 Hz, 1H), 5.47 (d, *J* = 15.2 Hz, 1H), 7.31–7.38 (m, 5H), 7.45 (d, *J* = 7.4 Hz, 1H), 7.49–7.51 (m, 1H), 7.55–7.58 (m, 1H), 7.61–7.63 (m, 1H), 7.66 (d, *J* = 8.2 Hz, 1H), 7.88 (s, 1H), 8.01 (dd, *J* = 8.2, 2.4 Hz, 2H), 9.73 (NH). ¹³C NMR (150.8 MHz, CD₃CN, 118.3 ppm, +25 °C) δ 50.5 (CH₂), 107.9 (Cq), 123.1 (CH), 126.7 (CH), 127.4 (CH), 128.0 (CH), 128.3 (CH), 128.7 (CH), 129.1 (CH), 129.3 (CH), 129.8 (CH), 129.9 (CH), 131.7 (Cq), 133.8 (Cq), 135.2 (Cq), 137.8 (Cq), 143.5 (CH), 149.5 (Cq), 152.1 (Cq), 156.7 (Cq). HRMS(ESI-QTOF). Calcd for C₂₂H₁₇N₄O₂⁺ 369.1346. Found 369.1345.

General Procedure for the Synthesis of Compounds 4–6. Products **1–3** (0.1 mmol) were dissolved in 2.5 mL THF and *t*-BuOK (18 mg, 0.16 mmol) followed by MeI (d = 2.28 g/mL, 0.01 mL, 0.16 mmol) were added. The mixture was stirred under reflux conditions for 2 h and after that, it was extracted with EtOAc. The combined organic layer was dried with Na₂SO₄, filtered and concentrated under reduced pressure to give the compounds **4–6** with 98% (white amorphous solid, 34 mg, 0.098 mmol), 97% (white solid, 36.5 mg, 0.097 mmol), 98% yield (white amorphous solid, 37.5 mg, 0.098 mmol), respectively.

7-Benzyl-3-methyl-1-(*o*-tolyl)-1H-purine-2,6(3H,7H)-dione (4). ¹H NMR (600 MHz, CD₃CN, 1.96 ppm, +25 °C) δ 2.06 (s, 3H), 3.51 (s, 3H), 5.48 (s, 2H), 7.13 (d, *J* = 7.8 Hz, 1H), 7.30–7.37 (m, 8H), 7.89 (s, 1H). ¹³C NMR (150.8 MHz, CD₃CN, 118.3 ppm, +25 °C) δ 17.5 (CH₃), 30.1 (CH₃), 50.6 (CH₂), 107.8 (Cq), 127.7 (CH), 128.8 (CH), 129.2 (CH), 129.6 (CH), 129.8 (CH), 130.2 (CH), 131.6 (CH), 136.7 (Cq), 137.6 (Cq), 137.8 (Cq), 143.1 (CH), 151.0 (Cq), 152.1 (Cq), 155.7 (Cq). HRMS(ESI-QTOF). Calcd for C₂₀H₁₉N₄O₂⁺ 347.1503. Found 347.1507. The atropisomers of compound **4** were resolved by ChiralPak AD-H column (5 μm, 250 × 20 mm, 20 mL/min, hexane:*i*PrOH = 80:20 v/v).

7-Benzyl-3-methyl-1-(2-nitrophenyl)-1H-purine-2,6(3H,7H)-dione (5). mp 176.0–179.0 °C, ¹H NMR (600 MHz, CD₃CN, 1.96 ppm, +25 °C) δ 3.52 (s, 3H), 5.45 (d, *J* = 15.4 Hz, 1H), 5.47 (d, *J* = 15.4 Hz, 1H), 7.32–7.38 (m, 5H), 7.49 (dd, *J* = 8.0, 1.4 Hz, 1H), 7.70 (td, *J* = 8.1, 1.4 Hz, 1H), 7.84 (td, *J* = 7.7, 1.5 Hz, 1H), 7.93 (s, 1H), 8.16 (dd, *J* = 8.2, 1.6 Hz, 1H). ¹³C NMR (150.8 MHz, CD₃CN, 118.3 ppm, +25 °C) δ 30.2 (CH₃), 50.8 (CH₂), 107.7 (Cq), 126.2 (CH), 128.7 (CH),

129.2 (CH), 129.8 (CH), 130.9 (Cq), 130.9₅ (CH), 133.2 (CH), 135.4 (CH), 137.5 (Cq), 143.7 (CH), 147.7 (Cq), 151.2 (Cq), 151.9 (Cq), 155.3 (Cq). HRMS(ESI-QTOF). Calcd for C₁₉H₁₆N₅O₄⁺ 378.1197. Found 378.1201. The atropisomers of compound **5** were resolved by Lux Cellulose 2 column (5 μm, 250 × 10 mm, 5 mL/min, hexane:iPrOH = 50:50 v/v).

7-Benzyl-3-methyl-1-(naphthalene-1-yl)-1H-purine-2,6(3H,7H)-dione (6). ¹H NMR (600 MHz, CD₃CN, 1.96 ppm, +25 °C) δ 3.56 (s, CH₃), 5.46 (d, J = 15.3 Hz, 1H), 5.49 (d, J = 15.3 Hz, 1H), 7.31–7.38 (m, 5H), 7.45 (d, J = 7.4 Hz, 1H), 7.47–7.51 (m, 1H), 7.54–7.58 (m, 1H), 7.61–7.64 (m, 1H), 7.65 (d, J = 8.2 Hz, 1H), 7.94 (s, 1H), 8.01 (dd, J = 8.2, 2.4 Hz, 2H). ¹³C NMR (150.8 MHz, CD₃CN, 118.3 ppm, +25 °C) δ 30.2 (CH₃), 50.6 (CH₂), 108.0 (Cq), 123.2 (CH), 126.7 (CH), 127.3 (CH), 127.9 (CH), 128.2 (CH), 128.7 (CH), 129.1 (CH), 129.3 (CH), 129.7₆ (CH), 129.8 (CH), 131.6 (Cq), 134.3 (Cq), 135.2 (Cq), 137.8 (Cq), 143.3 (CH), 151.2 (Cq), 152.6 (Cq), 156.2 (Cq). HRMS(ESI-QTOF). Calcd for C₂₃H₁₉N₄O₂⁺ 383.1503. Found 383.1504. The atropisomers of compound **6** were purified by ChiralPak AD-H column (5 μm, 250 × 20 mm, 20 mL/min, hexane:iPrOH = 76:24 v/v).

Compounds 7–9. See reaction scheme in Figure S2 of SI.

General Procedure for the Synthesis of Compounds 10–12.^{31,32} In a round-bottom flask equipped with a stir bar were added the appropriate isocyanate (8 mmol) in CHCl₃ (50 mL, 0.16 M), while stirring were added the appropriate aryl amine (12 mmol) and Et₃N (18.4 mmol, 2.6 mL). The mixture was stirred at room temperature from 3 h to overnight until complete disappearance of the isocyanate. The products were filtrated and washed with CHCl₃ and isolated as white precipitate.

1,2-Di-*o*-tolylurea (10, CAS Number: 617-07-2). Yield 93% (1.79 g, 7.45 mmol). ¹H NMR (400 MHz, DMSO-*d*₆, 2.54 ppm, +25 °C) δ 2.31 (s, 6H, CH₃), 6.98 (td, J = 7.5, 1.2 Hz, 2H), 7.14–7.24 (m, 4H), 7.84 (dd, J = 8.1, 0.9 Hz), 8.27 (bs, 2H, NH). ¹³C NMR (100 MHz, DMSO-*d*₆, 40.45 ppm, +25 °C) δ 18.9 (CH₃), 122.4 (CH), 123.6 (CH), 127.0 (CH), 128.6 (Cq), 131.1 (CH), 138.4 (Cq), 153.9 (CO).

1-(4-Methoxyphenyl)-3-(*o*-tolyl)urea (11, CAS Number: 106106-60-9). Yield 78% (1.6 g, 6.25 mmol). ¹H NMR (600 MHz, DMSO-*d*₆, 2.54 ppm, +25 °C) δ 2.23 (s, 3H, CH₃), 3.71 (s, 3H, CH₃), 6.87 (m, 2H), 6.92 (dd, J = 7.2 Hz, 7.2 Hz, 1H), 7.13 (dd, J = 7.9 Hz, 7.2 Hz, 1H), 7.16 (d, J = 7.2 Hz, 1H), 7.36 (m, 2H), 7.81 (s, 1H, NH), 7.83 (d, J = 7.9 Hz, 1H), 8.82 (s, 1H, NH). ¹³C NMR (150.8 MHz, DMSO-*d*₆, 40.45 ppm, +25 °C) δ 18.3 (CH₃), 55.6 (CH₃), 114.5 (CH), 120.2 (CH), 121.3 (CH), 122.8 (CH), 126.6 (CH), 127.7 (Cq), 130.6 (CH), 133.4 (Cq), 138.0 (Cq), 153.3 (Cq), 154.8 (Cq).

1-(4-Methoxyphenyl)-3-(naphthalen-1-yl)urea (12).³³ Yield 82% (1.92 g, 6.56 mmol). ¹H NMR (600 MHz, DMSO-*d*₆, 2.54 ppm, +25 °C) δ 3.73 (s, 3H, CH₃), 6.90 (m, 2H), 7.43 (m, 2H), 7.47 (dd, J = 8.0 Hz, 8.1 Hz, 1H), 7.54 (dd, J = 7.5 Hz, 7.3 Hz, 1H), 7.57–7.63 (m, 2H), 7.92 (d, J = 8.0 Hz, 1H), 8.04 (d, J = 7.3 Hz, 1H), 8.13 (d, J = 8.1 Hz, 1H), 8.69 (s, 1H, NH), 8.87 (s, 1H, NH). ¹³C NMR (600 MHz, DMSO, 40.45 ppm, +25 °C) δ 55.6 (CH₃), 114.5 (2CH), 117.6 (CH), 120.3 (2CH), 121.7 (CH), 123.1 (CH), 126.1 (CH), 126.2₇ (Cq), 126.3 (CH), 126.3₄ (CH), 128.9 (CH), 133.3 (Cq), 134.2 (Cq), 135.0 (Cq), 153.5 (Cq), 154.9 (Cq).

General Procedure for the Synthesis of Compounds 13–15.³⁴ In an oven-dried round-bottom flask purged with N₂ was dissolved the appropriate urea (10–12, 3.11 mmol) in anhydrous CHCl₃ (0.39 M, 8 mL); successively malonyl chloride (3.11 mmol, 0.3 mL) was added dropwise. The reaction mixture were refluxed for 5 h. After the solvent was removed in vacuo the crude solid was washed with *i*-PrOH until the mother liquors were clear of the product. The mother liquors were purified by a chromatographic column to afford products **13–15** as yellowish solids. A small sample for each product were purified by semipreparative HPLC for characterization purpose.

1,3-Di-*o*-tolylpyrimidine-2,4,6(1H,3H,5H)-trione (13, CAS Number: 184589-06-8). Compound **13** was prepared as described by the general procedure except the addition of 0.33 equiv of malonyl chloride (1.03 mmol, 0.1 mL) after 5 h and a longer reaction time (12 h). The product was purified by chromatographic column (DCM:MeOH = 95:5 with gradient to 90:10) to afford **13** with

92% yield (882 mg, 2.86 mmol). Further purification was performed by semipreparative HPLC on a Luna C18 column (5 μm, 250 × 21.2 mm, 20 mL/min, t_R = 5.45 min, ACN:H₂O = 70:30 v/v). ¹H NMR (600 MHz, CD₃CN, 1.96 ppm, +25 °C): Mixture **syn** 57.2% + **anti** 42.8% δ 2.22₉ (s, 6H, **syn**), 2.23₃ (s, 6H, **anti**), 3.98 (d, J = 21.2 Hz, 1H, **syn**), 4.00 (s, 2H, **anti**), 4.05 (d, 2H, J = 21.2 Hz, **syn**), 7.24–7.28 (m, 4H, **syn** + **anti**), 7.32–7.36 (m, 4H, **syn** + **anti**), 7.36–7.40 (m, 8H, **syn** + **anti**). ¹³C NMR (150.8 MHz, CD₃CN, 118.3 ppm, +25 °C): Mixture **syn** + **anti** δ 17.5 (CH₃), 17.6 (CH₃), 41.4 (CH₂), 41.6 (CH₂), 127.8₇ (CH), 127.9₁ (CH), 129.7 (CH), 129.7₅ (CH), 130.1₆ (CH), 130.1₇ (CH), 131.8 (2 CH), 135.3 (Cq), 135.4 (Cq), 137.5 (Cq), 137.8 (Cq), 151.9₈ (Cq), 152.0 (Cq), 166.3 (Cq), 166.3₄ (Cq).

1-(4-Methoxyphenyl)-3-(*o*-tolyl)pyrimidine-2,4,6(1H,3H,5H)-trione (14). Yield 91% (915 mg, 2.82 mmol). The compound was purified by chromatographic column on silica gel (DCM:MeOH = 95:5). Further purification was performed by semipreparative HPLC on a Luna C18 column (5 μm, 250 × 21.2 mm, 20 mL/min, t_R = 6.23 min, ACN:H₂O = 65:35 v/v). ¹H NMR (600 MHz, CDCl₃, 7.26 ppm, +25 °C) δ 2.18 (s, CH₃), 3.80 (s, CH₃), 3.94 (m, CH₂), 6.97 (m, 2H), 7.12 (m, 3H), 7.27–7.37 (m, 3H). ¹³C NMR (150.8 MHz, CDCl₃, 77.0 ppm, +25 °C) δ 17.4 (CH₃), 55.4 (CH₃), 40.2 (CH₂), 114.6 (CH), 126.2 (Cq), 127.1 (CH), 128.3 (CH), 129.2 (CH), 129.5 (CH), 131.1 (Cq), 133.1 (Cq), 135.6 (Cq), 150.3 (Cq), 159.8 (Cq), 164.0 (Cq), 164.7 (Cq). HRMS(ESI-QTOF). Calcd for C₁₈H₁₇N₂O₄⁺ 325.1183. Found 325.1188.

1-(4-Methoxyphenyl)-3-(naphthalen-1-yl)pyrimidine-2,4,6-(1H,3H,5H)-trione (15). Yield 92% yield (1.03 g, 2.86 mmol). The compound was purified by chromatographic column on silica gel (DCM:MeOH = 95:5 with gradient to 90:10). Further purification was performed by semipreparative HPLC on a Luna C18 column (5 μm, 250 × 21.2 mm, 20 mL/min, t_R = 5.82 min, ACN:H₂O = 60:40 v/v). ¹H NMR (600 MHz, CDCl₃, 7.26 ppm, +25 °C) δ 3.82 (s, CH₃), 4.12 (d, J = 22.0 Hz, 1H), 4.17 (d, J = 22.0 Hz, 1H), 6.99 (m, 2H), 7.21 (m, 2H), 7.41 (d, J = 7.4 Hz, 1H), 7.52–7.63 (m, 4H), 7.94 (d, J = 8.2 Hz, 1H), 7.97 (d, J = 7.8 Hz, 1H). ¹³C NMR (150.8 MHz, CDCl₃, 77.0 ppm, +25 °C) δ 40.5 (CH₃), 55.5 (CH₃), 114.7 (2CH), 121.0 (CH), 125.4 (CH), 126.2 (Cq), 126.6 (CH), 126.8 (CH), 127.5 (CH), 128.9 (CH), 129.3 (2CH), 129.7 (Cq), 130.1 (CH), 130.6 (Cq), 134.5 (Cq), 151.2 (Cq), 159.9 (Cq), 164.3 (Cq), 164.7 (Cq). HRMS(ESI-QTOF). Calcd for C₂₁H₁₇N₂O₄⁺ 361.1183. Found 361.1174.

General Procedure for the Synthesis of Compounds 16–18. In a test tube with a Teflon pressure-resistant cap was added the opportune bis-aryl barbituric acid (**13–15**, 2.80 mmol), H₂O (8.96 mmol, 160 μL), and slowly dropwise POCl₃ (19.6 mmol, 1.83 mL). Once the heat produced was dissipated the reaction mixture was refluxed overnight. The excess of POCl₃ was removed in vacuo and the reaction was quenched with ice. The aqueous phases were extracted with EtOAc (30 mL) five times. The combined organic layers were dried on Na₂SO₄, filtered and concentrated under reduced pressure. The crude were purified by chromatographic column and semipreparative HPLC.

6-Chloro-1,3-di-*o*-tolylpyrimidine-2,4(1H3H)-dione (16). Compound **16** was obtained starting from **13** (2.8 mmol, 863 mg). The product was purified by a chromatographic column on silica gel (petroleum ether:EtOAc 70:30) affording a yellow solid in 22% yield (201 mg, 0.616 mmol). Further purification was performed by semipreparative HPLC on a Luna C18 column (5 μm, 250 × 21.2 mm, 20 mL/min, t_R = 6.46 min, ACN:H₂O = 80:20 v/v with 0.05% HCOOH as acid modifier). ¹H NMR (600 MHz, CD₃CN, 1.96 ppm, +25 °C): Mixture **a** 57.0% + **b** 43.0% δ 2.18 (s, 3H, **b**), 2.19 (s, 3H, **a**) 2.25 (s, 3H, **b**), 2.27 (s, 3H, **a**), 7.24 (s, 1H, **b**), 7.25 (s, 1H, **a**), 7.33–7.46 (m, 16 H, **a** + **b**). ¹³C NMR (150.8 MHz, CD₃CN, 118.3 ppm, +25 °C) Mixture **a** + **b** δ 17.4₁ (CH₃), 17.4 (CH₃), 17.4₇ (CH₃), 17.4₈ (CH₃), 103.1 (CH) 103.1₄ (CH), 118.3 (CH), 127.9 (CH), 128.0 (CH), 128.2 (CH), 128.2₃ (CH), 129.5 (CH), 129.6 (CH), 130.0 (CH), 130.0₇ (CH), 130.1 (CH), 131.0₄ (CH), 131.0₅ (CH), 131.8 (CH), 132.0 (CH), 135.5₈ (Cq), 135.6 (Cq), 136.9 (Cq), 137.1₀ (Cq), 137.1₁ (Cq), 137.2 (Cq), 137.7 (Cq), 138.0 (Cq), 147.5 (Cq), 147.5₃ (Cq), 150.9 (Cq), 150.9₃ (Cq), 161.7 (Cq), 161.7₄ (Cq).

HRMS(ESI-QTOF). Calcd for $C_{18}H_{16}ClN_2O_2^+$ 327.0895. Found 327.0889.

6-Chloro-1-(4-methoxyphenyl)-3-(o-tolyl)pyrimidine-2,4(1H,3H)-dione (17a) and 6-Chloro-3-(4-methoxyphenyl)-1-(o-tolyl)pyrimidine-2,4(1H,3H)-dione (17b). The two regioisomers of compound 17 were obtained starting from 14 (2.8 mmol, 910 mg). The mixture was purified by a chromatographic column on silica gel (petroleum ether:EtOAc 70:30) affording a yellow solid in 48% yield (1.34 mmol, 460 mg). Further purification was performed by semipreparative HPLC on a Luna C18 column (5 μ m, 250 \times 21.2 mm, 20 mL/min, t_R = 7.91 min, ACN:H₂O = 70:30 v/v with 0.05% HCOOH as acid modifier). ¹H NMR (600 MHz, CDCl₃, 7.26 ppm, +25 °C) mixture a 60.3% + b 39.7% δ 2.20 (s, 3H, CH₃, a), 2.25 (s, 3H, CH₃, b), 3.82 (s, 3H, CH₃, a), 3.84 (s, 3H, CH₃, b), 6.15 (s, 1H, CH, b), 6.17 (s, 1H, CH, a), 6.98 (m, 4H, a + b), 7.15–7.24 (m, 8H, a + b), 7.28–7.39 (m, 8H, a + b). ¹³C NMR (150.8 MHz, CDCl₃, 77.0 ppm, +25 °C) mixture a + b δ 17.3₆ (CH₃), 17.4₄ (CH₃), 55.4 (CH₃), 55.5 (CH₃), 102.3₉ (CH), 102.4₄ (CH), 126.8 (Cq), 127.0 (CH), 127.2 (CH), 128.2 (CH), 128.8 (CH), 128.9 (C1), 129.1 (CH), 129.3 (CH), 129.9 (CH), 130.0 (CH), 131.1 (CH), 131.2 (CH), 133.7 (Cq), 135.5 (Cq), 135.6 (Cq), 136.3 (Cq), 146.4 (Cq), 147.0 (Cq), 150.4 (Cq), 150.5 (Cq), 159.7 (Cq), 160.3 (Cq), 160.5 (Cq), 161.2 (Cq). HRMS(ESI-QTOF). Calcd for $C_{18}H_{16}ClN_2O_3^+$ 343.0844. Found 343.0843.

6-Chloro-3-(4-methoxyphenyl)-1-(naphthalen-1-yl)pyrimidine-2,4(1H,3H)-dione (18a) and 6-Chloro-1-(4-methoxyphenyl)-3-(naphthalen-1-yl)pyrimidine-2,4(1H,3H)-dione (18b). The two regioisomers of compound 18 were obtained starting from 15 (2.8 mmol, 1010 mg). The mixture products 18 were purified by a chromatographic column on silica gel (petroleum ether:EtOAc 70:30) affording a yellow solid in 40% yield (1.12 mmol, 424 mg). Further purification was performed by semipreparative HPLC on a Luna C18 column (5 μ m, 250 \times 21.2 mm, 20 mL/min, t_R = 8.76 min, ACN:H₂O = 70:30 v/v with 0.05% HCOOH as acid modifier). ¹H NMR (600 MHz, CDCl₃, 7.26 ppm, +25 °C) mixture a 62.0% + b 38.0% δ 3.80 (s, 3H, CH₃, a), 3.84 (s, 3H, CH₃, b), 6.22 (s, 1H, CH, b), 6.25 (s, 1H, CH, a), 6.98 (m, 4H, a + b), 7.22 (m, 2H, a), 7.26 (m, 2H, b), 7.44 (d, J = 7.9 Hz, 1H, b), 7.48–7.65 (m, 9H, a + b), 7.68 (d, J = 8.5 Hz, 1H, b), 7.89–7.95 (m, 2H, a + b), 7.98 (d, J = 8.8 Hz, 1H, a). ¹³C NMR (150.8 MHz, CDCl₃, 77.0 ppm, +25 °C) mixture a + b δ 55.4 (CH₃), 55.5 (CH₃), 102.5 (CH), 102.6 (CH), 114.6 (2CH), 121.1 (CH), 121.4 (CH), 125.3 (CH), 125.5 (CH), 126.3 (CH), 126.5 (CH), 126.7 (Cq), 126.8 (CH), 127.3 (CH), 127.4 (CH), 128.0 (CH), 128.6₇ (CH), 128.7₄ (Cq), 128.8 (Cq), 129.2 (2CH), 129.5 (Cq), 129.7 (CH), 129.8 (CH), 129.9 (CH), 130.2 (Cq), 130.5 (CH), 131.2 (Cq), 132.8 (Cq), 134.3 (Cq), 134.5 (Cq), 147.0 (Cq), 147.3 (Cq), 150.8₇ (Cq), 150.8₉ (Cq), 159.7 (Cq), 160.2 (Cq), 160.9 (Cq), 161.2 (Cq). HRMS(ESI-QTOF). Calcd for $C_{21}H_{16}ClN_2O_3^+$ 379.0844. Found 379.0849.

General Procedure for the Synthesis of Compounds 19–21.

In a round-bottom flask were dissolved the opportune chloro-derivative (16–18, 0.61 mmol) in EtOH (1M, 0.61 mL) and were added CH₃NH₂ 40% aq (6.1 mmol, 0.47 mL). The reaction mixture were heated to reflux overnight. Once removed the EtOH at reduced pressure the crude was quenched with H₂O and extracted with EtOAc. The combined organic layers were dried on Na₂SO₄, filtered and concentrated. The crude products 19–21 were used without further purification in the next steps of the synthesis. Eventually a semipreparative HPLC purification were carried out in order to obtain analytically pure sample for characterization.

6-(Methylamino)-1,3-di-o-tolylpyrimidine-2,4(1H,3H)-dione (19).

Compound 19 was obtained as a yellow solid in 97% yield (0.59 mmol, 190 mg). Further purification was performed by semipreparative HPLC on a Luna C18 column (5 μ m, 250 \times 21.2 mm, 20 mL/min, t_R = 4.15 min, ACN:H₂O = 60:40 v/v with 0.05% HCOOH as acid modifier). Due to hindered rotation of the two aryl ring, two conformational diastereoisomer are present in a 61:39 mixture (a:b). ¹H NMR (600 MHz, DMSO-*d*₆, 2.54 ppm, +25 °C) δ 2.12 (s, 3H, a), 2.13 (s, 3H, b), 2.15 (s, 3H, a), 2.17 (s, 3H, b), 2.68 (s, 3H, a), 2.69 (s, 3H, b), 4.86 (m, 2H, a + b), 5.81–5.83 (m, 2H, a + b), 7.13–7.15 (d, 1H, J = 7.5 Hz, b), 7.16–7.17 (d, 1H, J = 7.5 Hz, a),

7.27–7.37 (m, 8H, a + b), 7.39–7.42 (m, 2H, a + b), 7.46–7.47 (m, 4H, a + b). ¹³C NMR (150.8 MHz DMSO-*d*₆, 40.45 ppm, +25 °C) mixture a + b δ 17.6 (CH₃), 17.7 (CH₃), 17.9 (CH₃), 18.1 (CH₃), 30.4 (CH₃), 73.9 (CH), 73.9₄ (CH), 127.3₃ (Cq), 127.3₄ (CH), 128.6 (CH), 128.9 (CH), 130.2 (CH), 130.2₃ (CH), 130.7 (Cq), 130.7₃ (CH), 130.7₆ (CH), 130.8 (CH), 131.1 (CH), 132.2₆ (CH), 132.3 (CH), 133.7 (Cq), 133.7₃ (Cq), 136.4 (Cq), 136.7 (Cq), 136.9 (Cq), 137.7 (Cq), 137.9 (Cq), 150.8 (Cq), 150.9 (Cq), 154.8 (Cq), 154.9 (Cq), 162.5 (Cq), 162.5₄ (Cq). HRMS(ESI-QTOF). Calcd for $C_{19}H_{20}N_3O_2^+$ 322.1550. Found 322.1544.

1-(4-Methoxyphenyl)-6-(methylamino)-3-(o-tolyl)pyrimidine-2,4(1H,3H)-dione (20a) and 3-(4-Methoxyphenyl)-6-(methylamino)-1-(o-tolyl)pyrimidine-2,4(1H,3H)-dione (20b). The mixture of compounds 20 were obtained as a yellow solid in 70% yield (0.427 mmol, 144 mg). Further purification was performed by semipreparative HPLC on a Luna C18 column (5 μ m, 250 \times 21.2 mm, 20 mL/min, t_R = 4.92 min, ACN:H₂O = 60:40 v/v with 0.05% HCOOH as acid modifier).

¹H NMR (600 MHz, CD₃CN, 1.96 ppm, +25 °C) mixture a 60.2% + b 40.8% δ 2.15 (s, 3H, CH₃, a), 2.18 (s, 3H, CH₃, b), 2.66 (m, 6H, N–CH₃, a + b), 3.82 (s, 3H, CH₃, a), 3.85 (s, 3H, CH₃, a), 4.60 (bs, 1H, NH, a), 4.71 (bs, 1H, NH, b), 4.83 (s, 1H, CH, b), 4.84 (s, 1H, CH, a), 6.98 (m, 2H, a), 7.10 (m, 2H, b), 7.16 (m, 4H), 7.25–7.32 (m, 6H), 7.30–7.46 (m, 2H). ¹³C NMR (150.8 MHz, CD₃CN, 118.3 ppm, +25 °C) mixture a + b δ 16.3 (CH₃), 16.7 (CH₃), 28.8₂ (CH₃), 28.8₄ (CH₃), 55.2 (CH₃), 55.4 (CH₃), 73.4₇ (CH), 73.5₃ (CH), 114.0 (CH), 115.4 (CH), 115.5 (CH), 126.5 (Cq), 126.6 (CH), 127.9 (CH), 128.3 (CH), 129.3 (CH), 129.4 (Cq), 129.8 (CH), 130.1₆ (CH), 130.1₈ (CH), 130.5 (CH), 130.9 (CH), 131.0 (CH), 131.7 (CH), 133.1 (Cq), 136.2 (Cq), 136.7 (Cq), 137.9 (Cq), 151.3 (Cq), 151.4 (Cq), 154.2 (Cq), 155.1 (Cq), 159.2 (Cq), 160.6 (Cq), 162.5 (Cq), 163.1 (Cq). HRMS(ESI-QTOF). Calcd for $C_{19}H_{20}N_3O_3^+$ 338.1499. Found 338.1493.

3-(4-Methoxyphenyl)-6-(methylamino)-1-(naphthalene-1-yl)pyrimidine-2,4(1H,3H)-dione (21a) and 1-(4-Methoxyphenyl)-6-(methylamino)-3-(naphthalene-1-yl)pyrimidine-2,4(1H,3H)-dione (21b). The mixture of compounds 21 were obtained as a yellow solid in 80% yield (0.487 mmol, 182 mg). Further purification was performed by semipreparative HPLC on a Luna C18 column (5 μ m, 250 \times 21.2 mm, 20 mL/min, t_R = 3.65 min, ACN:H₂O = 80:20 v/v with 0.05% HCOOH as acid modifier). ¹H NMR (600 MHz, CD₃CN, 1.96 ppm, +25 °C) mixture a 77.2% + b 22.8% δ 2.59 (d, J = 5.3 Hz, 3H, N–CH₃, a), 2.73 (d, J = 5.3 Hz, 3H, N–CH₃, b), 3.82 (s, 3H, CH₃, a), 3.85 (s, 3H, CH₃, b), 4.69 (bs, 1H, NH, a), 4.83 (bs, 1H, NH, b), 4.92 (s, 1H, CH, b), 4.93 (s, 1H, CH, a), 6.99 (m, 2H, a), 7.11 (m, 2H, b), 7.35 (m, 2H, b), 7.45 (d, J = 7.5 Hz, 1H, b), 7.55–7.69 (m, 8H, a + b), 7.80–7.85 (m, 2H, a + b), 7.99 (m, 2H, b), 8.06 (m, 2H, a + b), 8.11 (d, J = 8.2 Hz, 1H, a). ¹³C NMR (150.8 MHz, CD₃CN, 118.3 ppm, +25 °C) mixture a + b δ 29.5 (CH₃), 29.7 (CH₃), 56.0 (CH₃), 56.2 (CH₃), 74.3 (CH), 74.5 (CH), 114.8 (CH), 116.2 (CH), 116.3 (CH), 122.6 (CH), 123.3 (CH), 126.6 (CH), 127.0₇ (CH), 127.1₁ (CH), 127.2 (Cq), 127.7 (CH), 127.8 (CH), 127.9 (CH), 128.6 (CH), 129.1 (CH), 129.3₀ (CH), 129.3₄ (CH), 129.4 (CH), 130.1 (Cq), 131.0 (CH), 131.2 (CH), 131.4 (Cq), 131.6 (Cq), 131.7 (CH), 131.8 (CH), 134.6 (Cq), 135.0 (Cq), 135.7 (Cq), 152.6₀ (Cq), 152.6₄ (Cq), 155.5 (Cq), 156.1 (Cq), 160.0 (Cq), 161.4 (Cq), 163.8 (Cq), 164.0 (Cq). HRMS(ESI-QTOF). Calcd for $C_{22}H_{20}N_3O_3^+$ 374.1499. Found 374.1488.

General Procedure for the Synthesis of Compounds 22–24.

The appropriate methylamino derivative (19–21, 1 equiv, 0.4 mmol) and NaNO₂ (2 equiv, 0.8 mmol, 55 mg) were dissolved in H₂O (11.2 mL) and acetic acid (1.5 mL). The reaction mixture was left stirring at 0 °C overnight and the product was collected as a bright pink precipitate and washed twice with cold water. The mother liquors were eventually extracted with EtOAc to fully recover the product. The combined organic layers were dried on Na₂SO₄, filtered and the solvent was removed at reduced pressure. The crude product was used without further purification in the next steps of the synthesis. Eventually a semipreparative HPLC purification were carried out in order to obtain analytically pure samples for characterization.

6-(Methylamino)-5-nitroso-1,3-di-o-tolylpyrimidine-2,4-(1H,3H)-dione (22). The product **22** was obtained in 57.5% yield (gray amorphous solid, 0.23 mmol, 81 mg). Further purification was performed by semipreparative HPLC on a Luna C18 column (5 μ m, 250 \times 21.2 mm, 20 mL/min, t_R = 7.08 min, ACN:H₂O = 60:40 v/v with 0.05% HCOOH as acid modifier). Due to hindered rotation of the two aryl rings, two conformational diastereoisomers are present in a 57:43 mixture (a:b). ¹H NMR (600 MHz, DMSO-*d*₆, 2.54 ppm, +25 °C) δ 2.22 (s, 6H, a + b), 2.24 (d, 3H, *J* = 4.9 Hz, a), 2.25 (d, 3H, *J* = 4.9 Hz, b), 2.29 (s, 3H, a), 2.31 (s, 3H, b), 7.35–7.45 (m, 14H, a + b), 7.49–7.50 (m, 2H, a + b), 7.62 (d, 1H, *J* = 8.1 Hz, a), 7.70 (d, 1H, *J* = 8.1 Hz, b). ¹³C NMR (150.8 MHz, DMSO-*d*₆, 40.45 ppm, +25 °C) mixture a + b δ 17.9 (CH₃), 18.0 (CH₃), 18.1 (CH₃), 31.1 (CH₃), 31.1₅ (CH₃), 127.5₇ (CH), 127.6 (CH), 127.7₆ (CH), 127.8 (CH), 129.6₉ (CH), 129.7₁ (CH), 129.9₆ (CH), 130.0₁ (CH), 130.9 (CH), 131.0 (CH), 131.3 (CH), 131.4 (CH), 131.5 (CH), 131.7₇ (CH), 131.8₂ (CH), 135.0 (Cq), 135.1 (Cq), 135.2 (Cq), 135.3 (Cq), 135.7 (Cq), 137.2 (Cq), 138.7 (Cq), 139.0 (Cq), 139.5 (Cq), 139.6 (Cq), 147.8₆ (Cq), 147.9 (Cq), 149.4 (Cq), 149.4₄ (Cq), 160.2 (Cq), 160.3 (Cq). HRMS(ESI-QTOF). Calcd for C₁₉H₁₉N₄O₃⁺ 351.1452. Found 351.1444.

1-(4-Methoxyphenyl)-6-(methylamino)-5-nitroso-3-(o-tolyl)-pyrimidine-2,4-(1H,3H)-dione (23a) **3-(4-Methoxyphenyl)-6-(methylamino)-5-nitroso-1-(o-tolyl)pyrimidine-2,4-(1H,3H)-dione (23b).** The mixed products **23** were obtained in 50% yield (gray amorphous solid, 0.2 mmol, 73 mg). Further purification was performed by semipreparative HPLC on a Luna C18 column (5 μ m, 250 \times 21.2 mm, 20 mL/min, t_R = 5.88 min, ACN:H₂O = 50:50 v/v with 0.05% HCOOH as acid modifier). ¹H NMR (600 MHz, CD₃CN, 1.96 ppm, +25 °C) mixture a 60.0% + b 40.0% δ 2.23 (s, 3H, CH₃, a), 2.25 (d, 3H, *J* = 5.3 Hz N–CH₃, a), 2.29 (s, 3H, CH₃, a), 2.34 (d, 3H, *J* = 5.3 Hz N–CH₃, b), 3.85 (s, 6H, OCH₃, a + b), 7.05 (m, 4H, a + b), 7.29 (m, 3H, a + b), 7.34–7.49 (m, 7H, a + b). ¹³C NMR (150.8 MHz, CD₃CN, 118.3 ppm, +25 °C) mixture a + b δ 17.5 (CH₃), 17.8 (CH₃), 31.1 (CH₃), 31.8 (CH₃), 56.1 (CH₃), 56.3 (CH₃), 115.3 (CH), 115.5 (CH), 127.8 (CH), 128.0 (CH), 128.2 (Cq), 128.9 (CH), 129.8 (CH), 130.0 (CH), 130.8 (CH), 130.9 (CH), 131.5 (CH), 131.7 (CH), 132.1 (CH), 132.3 (Cq), 135.3 (Cq), 135.7 (Cq), 137.5 (Cq), 139.4 (Cq), 139.5 (Cq), 139.7 (Cq), 147.8 (Cq), 148.4 (Cq), 150.6 (Cq), 150.8 (Cq). HRMS(ESI-QTOF). Calcd for C₁₉H₁₉N₄O₄⁺ 367.1401. Found 367.1392.

1-(4-Methoxyphenyl)-6-(methylamino)-3-(naphthalen-1-yl)-5-nitrosopyrimidine-2,4-(1H,3H)-dione (24a) **and 3-(4-Methoxyphenyl)-6-(methylamino)-1-(naphthalen-1-yl)-5-nitrosopyrimidine-2,4-(1H,3H)-dione (24b).** The mixture of compounds **24** were obtained in 56% yield (gray amorphous solid, 0.224 mmol, 90 mg). Further purification was performed by semipreparative HPLC on a Luna C18 column (5 μ m, 250 \times 21.2 mm, 20 mL/min, t_R = 7.04 min, ACN:H₂O = 50:50 v/v with 0.05% HCOOH as acid modifier). ¹H NMR (600 MHz, CD₃CN, 1.96 ppm, +25 °C) mixture a 79.9% + b 20.1% δ 1.99 (d, *J* = 4.8 Hz, 3H, N–CH₃, a), 2.39 (d, *J* = 5.0 Hz, 3H, N–CH₃, b), 3.85 (s, 6H, CH₃, a + b), 7.06 (m, 2H, a), 7.35 (m, 2H, b), 7.48 (bs, 1H, b), 7.53 (bs, 1H, a), 7.60–7.70 (m, 3.8H, a + b), 7.75 (d, *J* = 8.0 Hz, 1H, a), 8.00 (m, 1H, b), 8.06 (m, 2H, a + b), 8.14 (d, *J* = 8.5 Hz, 1H, a). ¹³C NMR (150.8 MHz, CD₃CN, 118.3 ppm, +25 °C) mixture a + b δ 31.5 (CH₃), 32.2 (CH₃), 56.5 (CH₃), 56.7 (CH₃), 115.6 (CH), 115.8 (CH), 123.3 (CH), 123.6 (CH), 126.7 (CH), 127.1 (CH), 127.8 (CH), 128.3 (CH), 128.5 (CH), 129.2 (CH), 129.5₄ (CH), 129.5₆ (CH), 129.7 (CH), 129.9 (CH), 130.6 (CH), 131.1 (CH), 131.6 (Cq), 132.2 (CH), 132.5 (Cq), 132.7 (Cq), 133.0 (Cq), 133.6 (Cq), 135.2 (Cq), 135.5 (Cq), 140.0 (Cq), 148.8 (Cq), 151.5 (Cq), 161.0 (Cq), 161.7 (Cq), 162.1 (Cq). HRMS(ESI-QTOF). Calcd for C₂₂H₁₉N₄O₄⁺ 403.1401. Found 403.1386.

General Procedure for Compounds 7–9. The opportune nitroso-pyrimidine-dione (**22–24**, 1 equiv, 0.2 mmol) was refluxed for 3 h in 1 mL of DMF until complete disappearance of the bright pink color. Then to the reaction mixture cooled at room temperature was added K₂CO₃ (6 equiv, 1.2 mmol, 166 mg) and CH₃I (10 equiv, 2.00 mmol, 0.12 mL). Then the solution was heated at +50 °C for further 3 h. The work up proceeds with H₂O and extraction with EtOAc. The

combined organic layers were dried on Na₂SO₄, filtered and the solvent was removed at reduced pressure. The crude products were purified by semipreparative HPLC in high yields as separate isomers.

7-Methyl-1,3-di-o-tolyl-1H-purine-2,6(3H,7H)-dione (7). The mixture of **7a** and **7b** was obtained in ratio 45:55 respectively with overall 98% yield (white solid, 0.196 mmol, 68 mg, mp 213.3–215.5 °C). HRMS(ESI-QTOF). Calcd for C₂₀H₁₉N₄O₂⁺ 347.1502. Found 347.1493. The mixture of stereoisomers was resolved using ChiralPak AD-H column (5 μ m, 250 \times 20 mm, 20 mL/min, hexane:iPrOH = 80:20 v/v). **7a (trans)** ¹H NMR (600 MHz, CD₃CN, 1.96 ppm, +25 °C) δ 2.19 (s, 3H), 2.20 (s, 3H), 3.94 (s, 3H), 7.24–7.25 (m, 1H), 7.33–7.43 (m, 7H), 7.62 (s, 1H). ¹³C NMR (150.8 MHz, CD₃CN, 118.3 ppm, +25 °C) δ 17.5 (CH₃), 17.7 (CH₃), 34.0 (CH₃), 108.8 (Cq), 127.7 (CH), 127.9 (CH), 129.7 (CH), 130.2 (CH), 130.2₃ (CH), 130.2₄ (CH), 131.6 (CH), 131.9 (CH), 135.8 (Cq), 136.4 (Cq), 137.7 (Cq), 137.9 (Cq), 143.7 (CH), 150.2 (Cq), 151.3 (Cq), 156.0 (Cq). The atropisomers were resolved with t_R = 10.36 min and t_R = 11.41 min, respectively. **7b (cis)** ¹H NMR (600 MHz, CD₃CN, 1.96 ppm, +25 °C) δ 2.17 (s, 3H), 2.18 (s, 3H), 3.93 (s, 3H), 7.25–7.26 (m, 1H), 7.35–7.43 (m, 7H), 7.62 (s, 1H). ¹³C NMR (150.8 MHz, CD₃CN, 118.3 ppm, +25 °C) δ 17.4 (CH₃), 17.6 (CH₃), 34.0 (CH₃), 108.7 (Cq), 127.8 (CH), 128.0 (CH), 129.7 (CH), 130.1 (CH), 130.2 (CH), 130.2₅ (CH), 131.6 (CH), 131.9 (CH), 135.7 (Cq), 136.4 (Cq), 137.5 (Cq), 137.8 (Cq), 143.7 (CH), 150.2 (Cq), 151.3 (Cq), 156.1 (Cq). The atropisomers were resolved with t_R = 12.86 min and t_R = 17.89 min, respectively.

Compounds 8a and 8b. The mixture of **8a** and **8b** was obtained in ratio 42:58 respectively with overall 99% yield (white solid, 0.199 mmol, 72 mg, mp 204.5–205.3 °C). The two compounds were isolated by semipreparative HPLC on a Luna C18 column (5 μ m, 250 \times 21.2 mm, 20 mL/min, ACN:H₂O = 60:40 v/v) with t_R = 9.88 min (**8a**) and t_R = 9.34 min (**8b**).

3-(4-Methoxyphenyl)-7-methyl-1-(o-tolyl)-1H-purine-2,6(3H,7H)-dione (8a). ¹H NMR (600 MHz, DMSO-*d*₆, 2.54 ppm, +25 °C) δ 2.14 (s, 3H, CH₃), 3.85 (s, 3H, CH₃), 3.93 (s, 3H, CH₃), 7.08 (m, 2H), 7.27–7.41 (m, 6H), 8.01 (s, 1H). ¹³C NMR (150.8 MHz, DMSO-*d*₆, 40.45 ppm, +25 °C) δ 18.0 (CH₃), 34.1 (CH₃), 56.3 (CH₃), 108.0 (Cq), 115.1 (CH), 127.5 (CH), 128.8 (Cq), 129.3 (CH), 130.3 (CH), 130.7 (CH), 131.3 (CH), 136.1 (Cq), 137.0 (Cq), 143.9 (Cq), 150.2 (Cq), 151.2 (Cq), 155.2 (Cq), 159.9 (Cq). HRMS(ESI-QTOF) Calcd for C₂₀H₁₉N₄O₃⁺ 363.14517. Found 363.1462. The racemic mixture was resolved with ChiralPak AD-H column (5 μ m, 250 \times 20 mm, 20 mL/min, hexane:iPrOH = 72:28 v/v) with t_R = 10.04 min and t_R = 13.74 min.

1-(4-Methoxyphenyl)-7-methyl-3-(o-tolyl)-1H-purine-2,6(3H,7H)-dione (8b). ¹H NMR (600 MHz, DMSO-*d*₆, 2.54 ppm, +25 °C) δ 2.14 (s, 3H, CH₃), 3.83 (s, 3H, CH₃), 3.94 (s, 3H, CH₃), 7.04 (m, 2H), 7.26 (m, 2H), 7.37–7.43 (m, 6H), 7.99 (s, 1H). ¹³C NMR (150.8 MHz, DMSO-*d*₆, 40.45 ppm, +25 °C) δ 18.1 (CH₃), 34.1 (CH₃), 56.2 (CH₃), 108.0 (Cq), 114.9 (CH), 127.7 (CH), 129.3 (Cq), 129.8 (CH), 130.2 (CH), 131.2 (CH), 131.6 (CH), 135.5 (Cq), 137.2 (Cq), 143.9 (Cq), 149.4 (Cq), 151.3 (Cq), 155.9 (Cq), 159.7 (Cq). HRMS(ESI-QTOF) Calcd for C₂₀H₁₉N₄O₃⁺ 363.1452. Found 363.1456. The racemic mixture was resolved with ChiralPak AD-H column (5 μ m, 250 \times 20 mm, 20 mL/min, hexane:iPrOH = 72:28 v/v) with t_R = 10.91 min and t_R = 14.10 min.

Compounds 9a and 9b. The mixture of **9a** and **9b** was obtained in ratio 17:83 respectively with overall 99% yield (white solid, 0.198 mmol, 79 mg, mp 194.6–195.7 °C). The two compounds were isolated by semipreparative HPLC on a Luna C18 column (5 μ m, 250 \times 21.2 mm, 20 mL/min, ACN:H₂O = 35:65 v/v) with t_R = 18.58 min (**9a**) and t_R = 17.54 min (**9b**). Single enantiomers was separated by Lux Cellulose 2 column (5 μ m, 250 \times 10 mm), or ChiralPak AS-H column (5 μ m, 150 \times 4.6 mm, 50/50 *n*-hexane/iPrOH 0.6 mL/min).

3-(4-Methoxyphenyl)-7-methyl-1-(naphthalene-1-yl)-1H-purine-2,6(3H,7H)-dione (9a). ¹H NMR (600 MHz, CDCl₃, 7.26 ppm, +25 °C) δ 3.83 (s, 3H, CH₃), 4.01 (s, 3H, CH₃), 7.02 (m, 2H), 7.43 (m, 2H), 7.50 (m, 3H), 7.56 (s, 1H), 7.59 (dd, *J* = 8.3 Hz, *J* = 8.3 Hz, 1H), 7.69 (m, 1H), 7.94 (m, 2H). ¹³C NMR (150.8 MHz, CDCl₃, 77.0 ppm, +25 °C) δ 33.6 (CH₃), 55.5 (CH₃), 108.0 (Cq), 114.6 (CH), 121.6

(CH), 125.6 (Cq), 126.3 (CH), 127.0 (CH), 127.2 (CH), 127.3 (Cq), 128.7 (CH), 129.2 (CH), 129.4 (CH), 130.3 (Cq), 132.0 (Cq), 134.6 (Cq), 141.9 (CH), 149.8 (Cq), 151.2 (Cq), 155.5 (Cq), 159.7 (Cq). HRMS(ESI-QTOF) Calcd for $C_{23}H_{19}N_4O_3^+$ 399.1452. Found 399.1445. The racemic mixture was resolved with Lux Cellulose 2 column (32/68 *n*-hexane/*i*PrOH, 5 mL/min) with $t_R = 18.63$ min and $t_R = 31.20$ min, respectively. Kinetic studies were performed in ChiralPak AS-H column with $t_R = 16.85$ min and $t_R = 21.07$ min.

1-(4-Methoxyphenyl)-7-methyl-3-(naphthalene-1-yl)-1H-purine-2,6(3H,7H)-dione (9b). 1H NMR (600 MHz, $CDCl_3$, 7.26 ppm, +25 °C) δ 3.75 (s, 3H, CH_3), 3.94 (s, 3H, CH_3), 6.94 (m, 2H), 7.21 (m, 2H), 7.37 (s, 1H), 7.43 (m, 2H), 7.54 (m, 3H), 7.86 (d, $J = 8.5$ Hz, 1H), 7.92 (m, 1H). ^{13}C NMR (150.8 MHz, $CDCl_3$, 77.0 ppm, +25 °C) δ 33.6 (CH_3), 55.5 (CH_3), 107.8 (Cq), 114.6 (CH), 122.0 (CH), 125.6 (Cq), 126.5 (CH), 127.0 (CH), 127.3 (CH), 127.6 (Cq), 128.7 (CH), 129.7 (CH), 130.0 (CH), 130.1 (Cq), 131.4 (Cq), 134.7 (Cq), 142.1 (CH), 149.8 (Cq), 151.4 (Cq), 155.8 (Cq), 159.5 (Cq). HRMS(ESI-QTOF) Calcd for $C_{23}H_{19}N_4O_3^+$ 399.14517. Found 399.1447. The racemic mixture was resolved with Lux Cellulose 2 (40/60 *n*-hexane/*i*PrOH, 5 mL/min) column with $t_R = 40.65$ min and $t_R = 50.19$ min, respectively. Kinetic studies were performed in ChiralPak AS-H column with $t_R = 14.06$ min and $t_R = 21.22$ min, respectively.

■ ASSOCIATED CONTENT

Supporting Information

The Supporting Information is available free of charge on the ACS Publications website at DOI: 10.1021/acs.joc.7b01010.

Computational details for the conformational analysis of compounds 1–9; CSP-HPLC chromatograms for compounds 4–9; kinetic data for 7–9; Calculated ECD spectra for 4–9; 1H and ^{13}C NMR spectra for 1–9; computational data for 1–9 (PDF)

■ AUTHOR INFORMATION

Corresponding Authors

*E-mail: michele.mancinelli@unibo.it.

*E-mail: andrea.mazzanti@unibo.it.

ORCID

Michele Mancinelli: 0000-0002-8499-5265

Andrea Mazzanti: 0000-0003-1819-8863

Notes

The authors declare no competing financial interest.

■ ACKNOWLEDGMENTS

Financial contribution was received by A. M. from the University of Bologna (RFO funds 2015 and 2016). ALCHEMY Fine Chemicals & Research (Bologna, www.alchemy.it) is gratefully acknowledged for a generous gift of chemicals. Ms. Francesca Miglioli is gratefully acknowledged for technical assistance in the preparation of the compounds.

■ REFERENCES

- Christie, G. H.; Kenner, J. *J. Chem. Soc., Trans.* **1922**, 121, 614.
- Kuhn, R. In *Stereochemie, Deuticke, Leipzig*; Freudenberg, K., Ed.; 1933; pp 803–810.
- Okii, M. *Top. Stereochem.* **1984**, 14, 1–81.
- (a) Miyashita, A.; Yasuda, A.; Takaya, H.; Toriumi, K.; Ito, T.; Souchi, T.; Noyori, R. *J. Am. Chem. Soc.* **1980**, 102, 7932–7934. (b) Takaya, H.; Mashima, K.; Koyano, K.; Yagi, M.; Kumobayashi, H.; Taketomi, T.; Akutagawa, S.; Noyori, R. *J. Org. Chem.* **1986**, 51, 629–635.
- (a) Dos Santos, A. R.; Pinheiro, A. C.; Sodero, A. C. R.; da Cunha, A. S.; Padilha, M. C.; de Sousa, P. M.; Fontes, S. P.; Veloso, M. P.; Fraga, C. A. M. *Quim. Nova* **2007**, 30, 125–135. (b) Bringmann,

G.; Günther, C.; Ochse, M.; Schupp, O.; Tasler, S. *Prog. Chem. Org. Nat. Prod.* **2001**, 82, 1–249.

(6) Clayden, J.; Moran, W. J.; Edwards, P. J.; La Plante, S. R. *Angew. Chem., Int. Ed.* **2009**, 48, 6398–6401.

(7) (a) La Plante, S. R.; Edwards, P. J.; Fader, L. D.; Jakalian, A.; Hucke, O. *ChemMedChem* **2011**, 6, 505–513. (b) La Plante, S. R.; Fader, L. D.; Fandrick, K. R.; Fandrick, D. R.; Hucke, O.; Kemper, R.; Miller, S. P. F.; Edwards, P. J. *J. Med. Chem.* **2011**, 54, 7005–7022.

(8) Zask, A.; Murphy, J.; Ellestad, G. A. *Chirality* **2013**, 25, 265–274.

(9) Oğuz, S. F.; Doğan, İ. *Tetrahedron: Asymmetry* **2003**, 14, 1857–1864.

(10) (a) Kitagawa, O.; Fujita, M.; Kohriyama, M.; Hasegawa, H.; Taguchi, T. *Tetrahedron Lett.* **2000**, 41, 8539–8544. (b) Bennett, D. J.; Blake, A. J.; Cooke, P. A.; Godfrey, C. R. A.; Pickering, P. L.; Simpkins, N. S.; Walker, M. D.; Wilson, C. *Tetrahedron* **2004**, 60, 4491–4511. (c) Kitagawa, O.; Yoshikawa, M.; Tanabe, H.; Morita, T.; Takahashi, M.; Dobashi, Y.; Taguchi, T. *J. Am. Chem. Soc.* **2006**, 128, 12923–12931.

(11) (a) Shimizu, K. D.; Freyer, H. O.; Adams, R. D. *Tetrahedron Lett.* **2000**, 41, 5431–5434. (b) Bennett, D. J.; Pickering, P. L.; Simpkins, N. S. *Chem. Commun.* **2004**, 1392–1393.

(12) (a) Yilmaz, E. M.; Doğan, İ. *Tetrahedron: Asymmetry* **2008**, 19, 2184–2191. (b) Oppenheimer, J.; Hsung, R. P.; Figueroa, R.; Johnson, W. L. *Org. Lett.* **2007**, 9, 3969–3972.

(13) (a) Ciogli, A.; Kumar, S. V.; Mancinelli, M.; Mazzanti, A.; Perumal, S.; Severi, C.; Villani, C. *Org. Biomol. Chem.* **2016**, 14, 11137–11147. (b) Roussel, C.; Adjimi, M.; Chemlal, A.; Djafri, A. *J. Org. Chem.* **1988**, 53, 5076–5080.

(14) (a) Di Iorio, N.; Righi, P.; Mazzanti, A.; Mancinelli, M.; Ciogli, A.; Bencivenni, G. *J. Am. Chem. Soc.* **2014**, 136, 10250–10253. (b) Eudier, F.; Righi, P.; Mazzanti, A.; Ciogli, A.; Bencivenni, G. *Org. Lett.* **2015**, 17, 1728–1731. (c) Brandes, S.; Bella, M.; Kjærsgaard, A.; Jørgensen, K. A. *Angew. Chem., Int. Ed.* **2006**, 45, 1147–1151.

(15) Alkorta, I.; Elguero, J.; Roussel, C.; Vanthuynne, N.; Piras, P. *Adv. Heterocycl. Chem.* **2012**, 105, 1–188.

(16) CSD database, Sept. 2016. He, R.; Ching, S. M.; Lam, Y. J. *Comb. Chem.* **2006**, 8, 923–928.

(17) Casarini, D.; Lunazzi, L.; Mazzanti, A. *Eur. J. Org. Chem.* **2010**, 2010, 2035–2056.

(18) Lunazzi, L.; Mancinelli, M.; Mazzanti, A.; Lepri, S.; Ruzziconi, R.; Schlosser, M. *Org. Biomol. Chem.* **2012**, 10, 1847–1855.

(19) Chiarucci, M.; Ciogli, A.; Mancinelli, M.; Ranieri, S.; Mazzanti, A. *Angew. Chem., Int. Ed.* **2014**, 53, 5405–5409.

(20) Lunazzi, L.; Mazzanti, A. *J. Am. Chem. Soc.* **2004**, 126, 12155–12157.

(21) Diastereoisomers were equilibrated at +70 °C in $C_2D_2Cl_4$ for about 1 h. Starting from the two thermodynamically equilibrated diastereoisomers makes easier the kinetic treatment.

(22) Berova, N.; Di Bari, L.; Pescitelli, G. *Chem. Soc. Rev.* **2007**, 36, 914–931.

(23) Goel, A.; Kumar, V.; Hemberger, Y.; Singh, F. V.; Nag, P.; Knauer, M.; Kant, R.; Raghunandan, R.; Maulik, P. R.; Bringmann, G. *J. Org. Chem.* **2016**, 81, 10721–10732.

(24) (a) Mazzanti, A.; Mercanti, E.; Mancinelli, M. *Org. Lett.* **2016**, 18, 2692–2695. (b) Gunasekaran, P.; Perumal, S.; Menéndez, J. C.; Mancinelli, M.; Ranieri, S.; Mazzanti, A. *J. Org. Chem.* **2014**, 79, 11039–11050.

(25) Stonehouse, J.; Adell, P.; Keeler, J.; Shaka, A. J. *J. Am. Chem. Soc.* **1994**, 116, 6037–6038.

(26) Kupče, E.; Boyd, J.; Campbell, I. D. *J. Magn. Reson., Ser. B* **1995**, 106, 300–303.

(27) Frisch, M. J.; Trucks, G. W.; Schlegel, H. B.; Scuseria, G. E.; Robb, M. A.; Cheeseman, J. R.; Scalmani, G.; Barone, V.; Mennucci, B.; Petersson, G. A.; Nakatsuji, H.; Caricato, M.; Li, X.; Hratchian, H. P.; Izmaylov, A. F.; Bloino, J.; Zheng, G.; Sonnenberg, J. L.; Hada, M.; Ehara, M.; Toyota, K.; Fukuda, R.; Hasegawa, J.; Ishida, M.; Nakajima, T.; Honda, Y.; Kitao, O.; Nakai, H.; Vreven, T.; Montgomery, Jr., J. A.; Peralta, J. E.; Ogliaro, F.; Bearpark, M.; Heyd, J. J.; Brothers, E.; Kudin, K. N.; Staroverov, V. N.; Kobayashi, R.; Normand, J.; Raghavachari, K.;

Rendell, A.; Burant, J. C.; Iyengar, S. S.; Tomasi, J.; Cossi, M.; Rega, N.; Millam, N. J.; Klene, M.; Knox, J. E.; Cross, J. B.; Bakken, V.; Adamo, C.; Jaramillo, J.; Gomperts, R.; Stratmann, R. E.; Yazyev, O.; Austin, A. J.; Cammi, R.; Pomelli, C.; Ochterski, J. W.; Martin, R. L.; Morokuma, K.; Zakrzewski, V. G.; Voth, G. A.; Salvador, P.; Dannenberg, J. J.; Dapprich, S.; Daniels, A. D.; Farkas, O.; Foresman, J. B.; Ortiz, J. V.; Cioslowski, J.; Fox, D. J. *Gaussian 09*, Revision D.01; Gaussian, Inc.: Wallingford, CT, 2009.

(28) (a) Lee, C.; Yang, W.; Parr, R. G. *Phys. Rev. B: Condens. Matter Mater. Phys.* **1988**, *37*, 785–789. (b) Becke, A. D. *J. Chem. Phys.* **1993**, *98*, 5648–5652. (c) Stephens, P. J.; Devlin, F.J.; Chabalowski, C. F.; Frisch, M. J. *J. Phys. Chem.* **1994**, *98*, 11623–11627.

(29) *GaussView 5.0.9*; Gaussian Inc.: Wallingford, CT, 2009.

(30) (a) Bridson, P. K.; Wang, X. *Synthesis* **1995**, *1995*, 855–858. (b) He, R.; Lam, Y. *J. Comb. Chem.* **2005**, *7*, 916–920. (c) Zavalov, I. A.; Dahanukar, V. H.; Nguyen, H.; Orr, C.; Andrews, D. R. *Org. Lett.* **2004**, *6*, 2237–2240.

(31) Busschaert, N.; Kirby, I. L.; Young, S.; Coles, S. J.; Horton, P. N.; Light, M. E.; Gale, P. A. *Angew. Chem., Int. Ed.* **2012**, *51*, 4426–4430.

(32) Zhao, J.; Li, Z.; Yan, S.; Xu, S.; Wang, M.-A.; Fu, B.; Zhang, Z.; et al. *Org. Lett.* **2016**, *18*, 1736–1739.

(33) Zhao, J.; Li, Z.; Yan, S.; Xu, S.; Wang, M.-A.; Fu, B.; Zhang, Z. *Org. Lett.* **2016**, *18*, 1736.

(34) Whiteley, M. A. *J. Chem. Soc., Trans.* **1907**, *91*, 1330–1350.